Because the foil is a solid surface with no flow across it. Then we know that the circulation set up in the boundary layer is not able to cause flow into the foil, rather by superposition, the sum of the flow induced by the local vortex flow, dv_v, determined by the magnitude of γ(x), must be balanced by the freestream flow component normal to the foil surface (which is at angle α to the freestream if we neglect the small camber for now). Since these two velocities must balance yielding no flow across the foil, then the vortex induced velocity can be written as:

$$dv_v = U \sin\alpha$$

Note that the vortex induced velocity is given by $\gamma(x)dx = 2\pi r dv_v$, where r is the distance from the center of the vortex to some point along the foil surface. To get the entire induced velocity integration is required along the entire foil chord length, c. This can be expressed, for a flat airfoil at an angle of attack of α as:

$$\int_0^c dv_v = \int_0^c \frac{\gamma(x)}{2\pi r} dx$$

The above integral would need to be evaluated along the foil containing a line distribution of vortices given by γ(x) to find the induced velocity at any point on the foil. To do this the variable position "r" needs to be expressed in terms of the coordinate x, measured along the chord line. If we select a position on the foil, x_o , that designated a given location of a vortex sheet element then $r = (x_o - x)$. Using the above expression for dv_v in terms of $U \sin\alpha$ we obtain an integral equation for the distribution of local circulation:

$$U \sin\alpha = \int_0^c \frac{\gamma(x)}{2\pi(x_o - x)} dx \tag{6.19}$$

The above condition needs to be satisfied for the given distribution $\gamma(x)$ along the foil. However, we need a boundary condition at $x = c$ that specifies $\gamma(c)$. This is done by introducing what is known as the Kutta Condition. This is based on the observed flow condition at the trailing edge of the foil, assuming the geometry is such that the flow from the top and bottom sides meet at a point (the trailing edge) and that flow exits the foil "smoothly" from the top and bottom surfaces such that there is no vorticity as the flow leaves the trailing edge. Physically this would occur if there is no roll-up of the flow say from the bottom to the top surface. If the velocities on top and bottom at the trailing edge are identical, then the pressures are identical by the Bernoulli equation, and the flow has no tendency to swirl. So, this condition is expressed as $\gamma(x = c) = 0$. It can then be shown that the integration in Eqn. (6.19) is found to satisfy the Kutta Condition for the following distribution of the vortex sheet:

$$\gamma(x) = 2U \sin\alpha(c/x - 1) \tag{6.20}$$

(See the extra comments on the Kutta condition below.)

With this distribution of $\gamma(x)$ the total circulation, Γ, can be determined. Note that this value of Γ depends on the angle of attack, α, and the free stream velocity, U. We can now use the previously given result that the lift force, L , is dependent on the circulation that was shown for a rotating cylinder in a freestream, $L = \rho U \Gamma$. This is further discussed below and is found to be valid for airfoils in irrotational flow.

The integration of $\gamma(x)$) given in Eqn. (6.19) results in the following Lift expression for an airfoil:

$$L = 2\pi \sin \alpha \rho U^2 c$$

Or by defining the nondimensional lift coefficient as the lift force divided by $1/2 \rho U^2$:

$$C_L = 2\pi \sin \alpha \tag{6.21}$$

This surprisingly simple expression is a major finding of the thin air foil theory in the description of the lift force as determined by the foil angle of attack. This is based on a two-dimensional steady flow (or infinitely wide foil) with very little camber with viscous effects ignored. Some additional features and effects will be added to this equation later. Figure 6.7, shows the lift coefficient versus angle of attack. At large angles of attack the results of eqn. (6.21) are not valid. This is because the angle is so large that flow over the leading edge cannot negotiate the needed turn to stay "attached" to the foil surface. Rather the flow "separates" from following the surface contour. This results in a recirculating flow region between the streamlines of flow and the body surface. This can be seen in Fig. 4.5 illustrating flow going over the leading edge of a thin airfoil at a fairly large angle of attack.

The primary limitation on the application of thin airfoil theory is the assumption of inviscid flow (which is actually has been shown to be a fairly valid approximation since all of the friction induced vorticity is accounted for with the vortex sheet). Also, the foil must be thin (maximum thickness on the order of ten percent of the chord length). This is not necessarily that restrictive since even airfoils with thicknesses of over 10% of the chord follow thin airfoil theory fairly well. With some modifications to the basic lift result of Eqn. (6.19) thickness effects, relatively large camber and three-dimensional effects can be accounted for, as given below. A generic plot of the lift coefficient, C_L, versus angle of attack, a, is given in Fig. 6.7, as well as results for a specific airfoil, the NACA 0012 compared with Eqn. (6.21). Very good agreement between data and theory are shown up to an angle of attack of about 16$^{\text{o}}$.

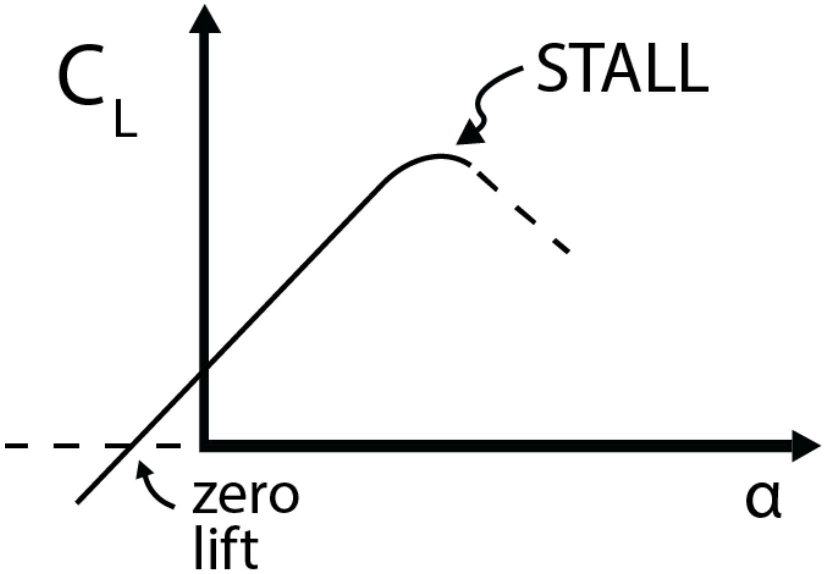

Fig 6.7 Illustration of a typical Lift coefficient versus angle of attack curve, left, and comparison with Eqn. (6.19) and data for a NACA 0012 air foil.

The Kutta Condition

(See this website [en.wikipedia.org/wiki/Kutta_condition].)

As mentioned above a boundary condition was needed in order to complete the thin airfoil theory to determine ultimately the lift force on an airfoil. This is known as the Kutta condition and is applied to airfoils when describing the external flow around the foil to provide an inviscid condition that is linked to the viscous flow effect at sharp corners on an object. First consider inviscid flow over a cylinder (two-dimensional flow). In such a flow there is no separation and there is a stagnation point on the upstream side of the cylinder and a similar stagnation point on the downstream side of the cylinder. In fact, by observing streamlines it is not apparent which is the upstream and downstream side of the cylinder since the streamlines, and the flow in general is symmetric. This symmetric flow results in a symmetric pressure field around the cylinder such that the drag and lift forces are identically zero. If the object is changed to be an oval the flow again has two stagnation points, and when the oval major axis does not align with the flow direction there is also two stagnation points that do not align with the major axis.

Now consider the case of an airfoil, with a rounded leading edge and a very sharp trailing edge. If the airfoil has a slight positive angle of attack then the upstream stagnation point occurs on the lower surface of the airfoil. The downstream stagnation point will want to move to the topside of the airfoil surface as for an oval shape. But in doing this the flow must go around the sharp trailing edge which has a near zero radius of curvature. Consequently, the velocity required to go around this corner tends towards infinity. In reality viscous effects acting on this high velocity region prevent the occurrence of this very large velocity. The Kutta condition accounts for this by forcing the velocity on the upper and lower surface to be identical at the tip of the sharp trailing edge. This results in a zero pressure gradient across the flow at the trailing edge as well. If the airfoil were to start from rest and suddenly accelerate within a fluid at rest then the flow would role-up behind the trailing edge forming a vortex whose strength depends on the acceleration. This shed vortex leaves the airfoil as the airfoil moves, this is known as the "starting vortex".

By Kelvin's theorem for an inviscid fluid there cannot be any change in total vorticity within a fluid region so the airfoil must carry with it a "bound" vorticity equal and opposite in sign to the starting vorticity. Since circulation is the spatial integral of vorticity then it can be said that the airfoil has circulation, which can be shown to be proportional to the lift force generated on the airfoil by the Kutta-Joukowski theorem. What is left is a stagnation point at the trailing edge of the airfoil as the flow from the top and bottom surfaces come together, similar to the flow from the top and bottom of the original cylinder discussed earlier. The fluid leaving the top and bottom surfaces flows parallel with each other with equal magnitude. This is a convenient physical flow condition that is often used in many flow conditions to provide mathematical closure.

Circulatory Lift: A Simple Method to Define Lift for an Airfoil

In this section we present an alternative approach to determining the lift for an airfoil. Consider a two-dimensional steady flow (a very wide airfoil) with the goal of determining the lift force versus angle of attack. There are much more rigorous methods to do this, involving complex variable representation of the flow. However, this simple treatment is rather straight forward and yields the same result in a more intuitive manner. The goal here is to illustrate from a flow physics point of view how the circulation is related to the lift force, and without circulation the lift force vanishes.

The no-slip boundary condition at the surface of the airfoil generates vorticity along the surface of the wing. For a perfectly symmetric wing that is oriented along the incoming flow direction the streamlines above and below the foil are identical. One can also imagine that the vorticity distribution on the top of the wing generated by surface friction is identical in magnitude but opposite in sign on the bottom of the wing (the rotation direction is opposite). Consequently, the sum total of vorticity around the wing becomes zero for this situation. However, tilting the wing at a given angle of attack relative to an in-coming flow creates an asymmetry of flow. See Fig. 6.8 below. Notice in the figure that the flow leaves the trailing edge of the wing with a net downward flow direction either due to the camber or a tilting of the chord line relative to the freestream flow direction. In fact, in a vector sense the downward momentum of the flow has to have been generated by some downward force acting on the fluid. Selecting a rectangular control volume surrounding the wing and using this to integrate the velocity field along the surface of the control volume area as shown determines the magnitude of the circulation as:

$$\Gamma = \oint V \bullet ds = \iint_A \omega \bullet dA$$

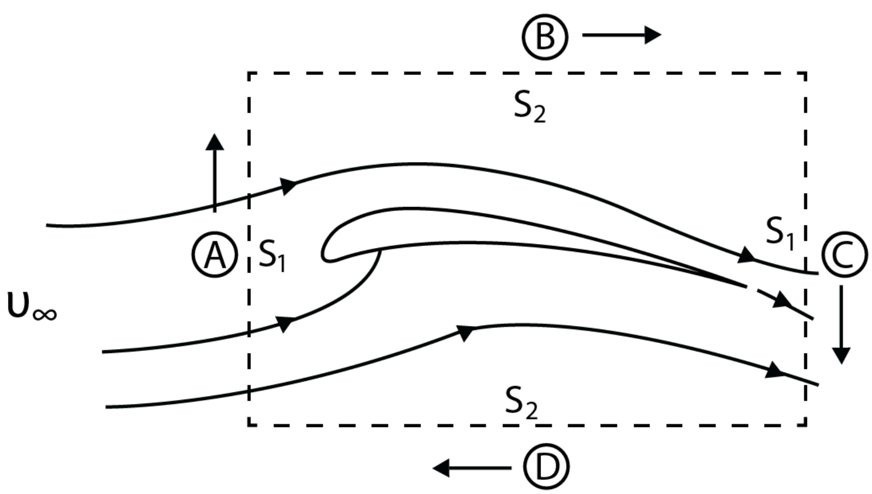

Fig 6.8 Illustration of the streamlines associated with flow over a cambered airfoil producing asymmetric flow with a freestream velocity of [latex]U_\infty[/latex]; a control volume analysis is used with sides A, B, C and D.

Where the line integral of the velocity is around the boundary of the area associated with the area of the vorticity integral. The contributions to the line integral for the different sides of the area are:

A: = 0 (there is no velocity component along this length (dot product of V and ds is zero)

B: ~$U_\infty S_2$ (the boundary is far from the wing surface so the velocity is close to U_∞)

C: ~$Ws1S_1$ (W is the downward velocity component of the flow coming off of the trailing -edge which is assumed to be parallel with the top of the airfoil)

D: ~$-U_\infty S_2$ (negative since the velocity is in the opposite direction as the integration)

By summing these components to obtain the total integration becomes $\Gamma = WS_1$. This shows that the circulation is equal to the amount of downflow generated as the flow passes the airfoil. The lift force on the wing is equal and opposite to the force on the fluid. Using the momentum equation to determine the relationship between the force on the fluid and the change of momentum of the fluid results in (where forces are primed to represent force per span into the page):

$$F' = L' = \dot{m}W = (\rho S_1 U_\infty)W = (\rho U_\infty)\Gamma$$

This illustrates that any object generating a downflow velocity in the control region will result in a net lift force on the object balancing the change of momentum of the fluid in the vertical direction. Also, this force is seen to be directly proportional to the circulation set up around the object. The assumption here is of irrotational flow outside of the viscous boundary layer so that there are no other sources of vorticity inside the selected control volume.

A slightly modified version of this can be used to determine the lift coefficient as well. Imaging a circle drawn around the wing with its center at the center of the wing (radius of $c/2$, where c is the chord length). With this radius the circle will pass through the leading edge and trailing edge. Performing the line integral of the velocity component aligned with the circumference of the circle (dotting the velocity with ds) around the entire circle and using the notation of "W" being the net velocity component downward around the circle results in:

$$\Gamma = \oint V \bullet ds = W \oint ds = W 2\pi \left(\frac{c}{2}\right) = \pi c W$$

The lift force per span is then

$$L' = \rho s U_\infty (\pi c W)$$

The lift coefficient is the lift force per area (sc) divided by

$$\frac{1}{2}\rho\, {U_\infty}^2 : C_L = \frac{L\prime}{1/2\rho {U_\infty}^2} = \frac{2\pi W}{U_\infty}$$

The ratio of the downwash velocity to the freestream velocity can be estimated as sin α, with a being the angle of attack, which results in:

$$C_L = 2\pi \sin \alpha \sim 2\pi\alpha \text{ (for small angle } \alpha\text{)}$$

This is the same result obtained using the more rigorous thin airfoil theory which helps to provide some physical insight into the role of the airfoil in defecting flow to obtain a net lift force.

Other Considerations of Forces

As stated previously the lift force is one component of the total force, the other component being the drag force. The drag force, D, can be expressed as a drag coefficient, $C_D = D/(1/2\rho U^2 sc)$, similar to the lift coefficient. Although the drag force varies with angle of attack, unlike the lift coefficient it is fairly constant for a wide range of angle of attack prior to separation as shown in the figure below, except at fairly large angle of attack approaching the stall limit. Near zero angle of attack for a symmetric airfoil this drag is dominated by frictional forces acting on the foil surface. Another representation for the lift and drag coefficient is a "polar" plot which shows how the lift coefficient changes with drag coefficient. An example is shown below where the tangent line provides the minimum lift to drag ratio.

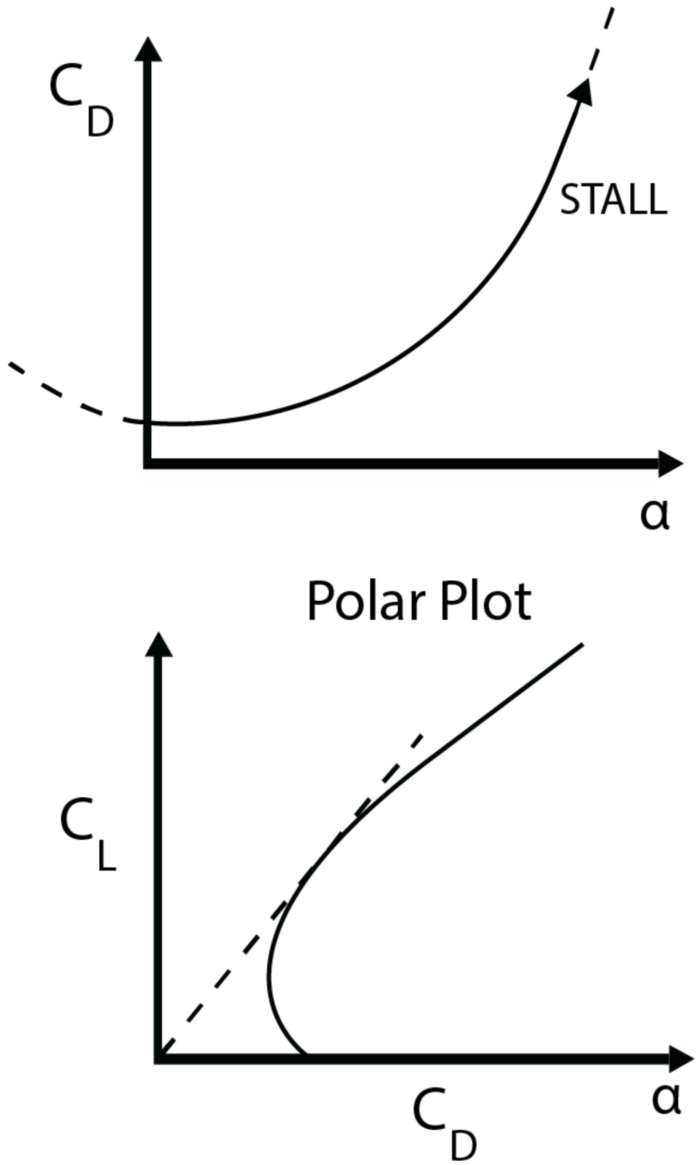

Fig 6.9 Illustration of a typical airfoil drag coefficient, [latex]C_D[/latex], versus angle of attack, top, and lift coefficient versus drag coefficient, known as a polar plot.

As stated previously there may be effects on the lift and drag forces caused by finite span (three-dimensional) wings, thickness and camber that would need to be taken into account. Finite span wings are obviously a reality and the fact that the ends of the wing (wing tips) causes flow conditions in the tip region to change. Specifically, the high pressure that exists below the wing meets with the low pressure on the top of the wing creating the tendency for a tip vortex to form. The resultant flow is a swirling flow directed from the bottom to the top of the wing. This appears as a vortex flow whose axis of rotation aligns closely with the direction of the freestream velocity. As the wing moves through the fluid the vortex axis extends out behind the wing. In fact, this phenomena for airplanes flying at sufficiently high altitudes the vortex motion results in a very low pressure at the center of the tip vorticities. The drop in pressure can cause water vapor to condense resulting in vapor trails or contrails forming at the wing tips that can be seen on the ground as a plan passes overhead. This phenomenon does have some negative effects on the performance of the wing.

The span of a wing determines how significant the tip vortex is on overall forces. A wing can be designated based on its span to chord length ratio (or aspect ratio). The term wing span of an aircraft typically includes the distance from tip to tip of the wings on an airplane – or twice the span of each wing. For a given wing however, the span is from the root to the tip. Denoting span by "s" and chord by "c" the aspect ratio is then s/c. The swirling flow that results near the tip has flow coming up from the bottom, around the tip and then down onto the top of the wing. This downflow will have a tendency to divert the oncoming flow over the wing downward such that there is effectively a smaller angle of attack as seen by the wing. The axis of the vortex near the tip is characterized by the vortex line shown in the figure below extending backwards from the tip. In addition to this a "bound" vortex occurs around the wing due to the previously discussed vorticity distribution, with an axis of rotation along the wing span.

An induced angle of attack is defined as the amount of change (reduction) of the angle of attack as caused by the top vortex:

$$\alpha_{eff} = \alpha - \alpha_{induced}$$

The strength of $\alpha_{induced}$ is given in terms of the downflow velocity induced by the tip vortex as:

$$\alpha_{induced} = tan^{-1}\frac{W}{U_\infty}\ \frac{W}{U_\infty}$$

Where the later approximation is due to small angles since $W << U_\infty$. Shown here without derivation, the total circulation accounting for the downwash effect written in terms of α_{eff} is:

$$\Gamma = \pi c U_\infty \alpha_{eff}$$

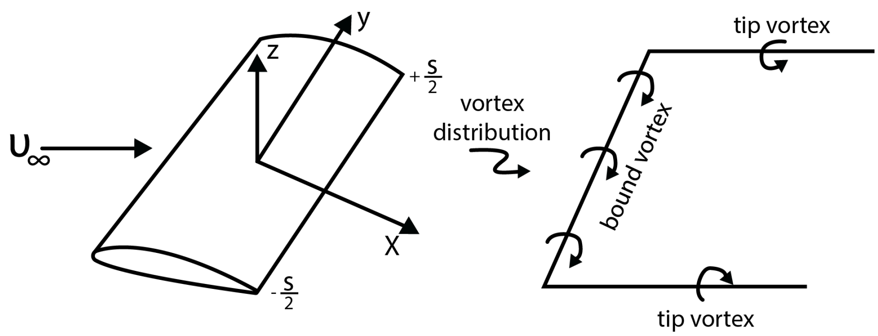

Fig 6.10 Illustration of the vortex distribution for a finite length wing; lines represent the vortex axis of rotation.

Using this expression for the circulation to determine the lift after some manipulation the lift coefficient becomes:

$$C_L = \frac{2\pi\alpha}{1 + \frac{2c}{s}}$$

In the limit of large aspect ratio, or c/s becoming small, the lift coefficient reverts to that for an infinite span wing as expected. Also, there is an induced drag that is set up from the downflow which can be determined in terms of the lift coefficient to be:

$$C_{D,\ induced} = \frac{{C_L}^2}{\pi s/c}$$

$$C_D = C_{Do} + C_{D,\ induced}$$

where $C_{D,o}$ is the drag coefficient for an infinite wing.

There is also an effect caused by asymmetry in the foil geometry such as camber. In this case the camber adds to the asymmetry of the foil as shown in Fig. 6.6. The maximum camber along the chord line is designated as "h" and the maximum thickness as "t".

For cambered foils the lift becomes:

$$\Gamma = \pi s U_\infty \left(1 + 0.77\frac{t}{c}\right) \sin\left(\alpha + \beta\right)$$

$$\beta = tan^{-1}\left(\frac{2h}{c}\right)$$

As the camber increases, by increasing h/c, and therefor increasing β, the circulation increases. Using this to define the lift coefficient we have the following relationship that accounts for both finite span wings and camber asymmetry:

$$C_L = 2\pi\left(1 + 0.77\frac{t}{c}\right)\sin\left(\alpha + \beta\right)/\left(1 + \frac{2c}{s}\right)$$

The effect of an artificially imposed camber is shown in the figure below by using a flap at the rear of the foil. There can be a significant increase in lift when deploying a flap, and this provides a means to increase lift as needed.

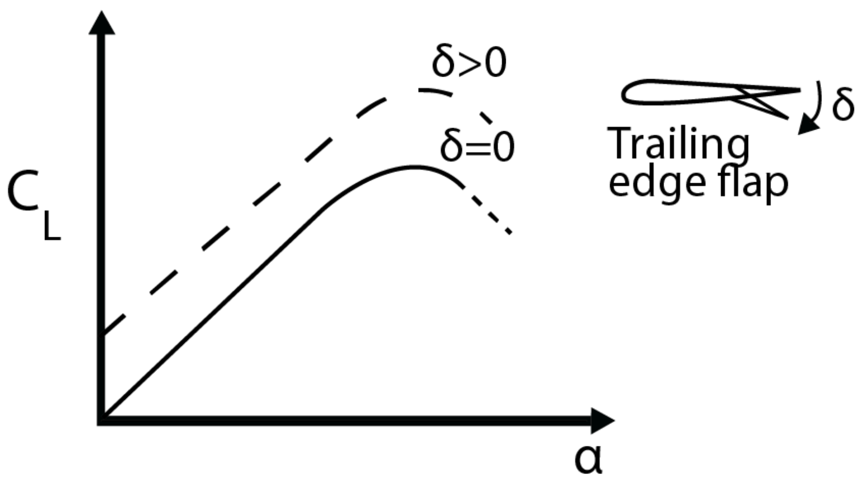

Fig 6.11 Effect of a trailing edge flap to provide effective camber and increased lift.

Airfoil shapes are often designated by different “codes” or “designations”. An early form of this was developed by NACA (National Advisory Committee for Aeronautics, a precursor to NASA). Several such designations have been developed such as the 4, 5 and 6 digit numerical designations as are shown below based on camber, location of maximum camber and thickness. More elaborate designations have been developed over the years.

NACA DIGIT Airfoil Designation

Four Digit: a b c d

a: maximum camber % of chord, c

b: location of maximum camber from leading edge, tenths of c

c & d: maximum thickness, % of c

Example: NACA 2412: max camber is 0.02c; location is 0.4c from leading edge and max thickness is O. l 2c.

Five Digit: a b c d e

a: multiple by 2/3 = design lift coefficient in tenths

b & c: divided by 2 = location of maximum camber from leading edge in %c

d & e: maximum thickness in % of c

Example: NACA 2412: design lift coefficient is 0.3; location of max camber is 0.15c, max thickness is O. l 2c.

Six Digit: a b c d e f

a & b: series designation

c: location of minimum pressure in tenths of c from leading edge

d: design lift in tenths

e & f: maximum thickness in % of c.

VII. INTRODUCTION TO VISCOUS FLOWS

In this section we develop the governing equations for viscous flows resulting in the Navier-Stokes equations. We will simplify the equations for incompressible constant property flows, which are useful for a vast majority of flow situations. We will then show how this seemingly formidable set of equations can be simplified for a number of rather practical flow problems resulting in exact, analytical solutions. We end with the introduction to similarity solutions to the Navier-Stokes equations through an example problem.

Basics of Viscous Forces

The introduction of viscous forces requires a model to obtain a set of conditions on the flow field to express the viscous stress tensor, τ_{ij}, as a function of the local velocity field. This stress tensor consists of the various stresses that can occur on an element of fluid. These forces act at the surface of a fluid element and are caused by a velocity gradient normal to the surface. This velocity gradient can give rise to local friction. In regions of the flow where the velocity gradients go to zero we expect there to be no viscous forces acting. We will show that even though viscous forces may not be zero due to existing velocity gradients their net effect may in fact be zero on a fluid element when taking into account all viscous forces over all the surfaces of an element. Additionally, it is possible to have velocity gradients and no net viscous forces. This will be evident once we present a model equation describing the viscous forces.

By including viscous forces in the flow we need to introduce the no-slip boundary condition, whereby the fluid in contact with a surface takes on the same velocity as the surface — the fluid is not allowed to "slip" along the surface. In doing this a velocity profile is set up across the flow direction. For example in pipe flow the fluid velocity at the pipe wall is the same as the velocity of the pipe, but to have a net flow through the pipe fluid away from the wall is moving differently than the pipe. If the pipe is circular the center of the pipe is furthest from the walls and the fluid in this portion of the pipe is traveling fastest. So for a circular pipe the flow is symmetric circumferentially with a maximum in the center. For pipes with different cross sections we still expect a peak velocity in the region furthest from all walls, since the impact of the wall friction is furthest away. Friction occurs throughout the cross section however, not just at the walls. This internal friction is fluid-fluid friction due to the fact that different "layers" of fluid, or fluid elements are moving at different velocities.

For laminar pipe flows, which most readers have seen in their first course in fluid mechanics, there are some characteristic conditions we can discuss that are relevant to internal viscous flows in general. In the case of steady, fully developed flow we can set a force balance to better understand the required forces acting on the fluid. We will define this characterization of the flow (steady, fully developed) in a later part of this chapter, in reference to the governing equation. Referring to Fig. 7.1 (a) for the illustrated control volume of length dx extending across the area of the round pipe of radius R we see that a force balance for nonaccelerating flow between the force due to pressure and that due to wall friction becomes:

$$\frac{dP}{dx} = -\frac{2\pi R}{\pi R^2}\tau_w = -\frac{2\tau_w}{R} \tag{7.1}$$

This indicates that the pressure decreases along the flow direction proportional to the magnitude of the wall shear stress caused by friction between the fluid and pipe wall. In this equation the values of the wall shear stress is taken as a positive number.

External flows have a similar no-slip condition at a surface, the difference being that as one moves away from the surface any other boundaries are "infinitely" far away in the sense that these other surfaces are not influencing the flow. This is shown in Fig. 7.1 (b) showing that the extent of the friction layer increases along the flow direction. However, there is still wall friction and fluid-fluid friction up to some point far enough from the surface, which depends on the particular location along the surface. We will discuss this in detail when we examine boundary layer flows. Recall that in previous sections we neglected viscous effects for external flows and the results tend to be very accurate, this is because for the flows we looked at other forces that come into play (pressure and body forces) dominate the flow. However, even in these flows viscous forces can be important in that they lead to "flow separation" where streamlines no longer follow the general shape of the object. When this occurs the potential flow solutions tend to break down, even though pressure forces dominate the overall forces. This is because the velocity distribution is greatly altered by the flow separation. This topic of flow separation is beyond the scope of this book but we will discuss it to a limited extent in the next chapter. The reader is referred to "Viscous Fluid Flow" by F.M. White for a discussion of this and some of the many models used in these flows, to predict wall friction effects.

The velocity profiles shown in Fig. 7.1 indicates a variation of velocity from the boundary condition at the surface of no-slip to a maximum at the centerline for pipe flow or reaching the freestream velocity far from the surface in external flows. This implies a distribution of internal viscous stress caused by the local velocity distribution since frictional forces depend on the relative velocity variation, or velocity derivative, within the flow field. In order to determine the magnitude of these forces we will first define the viscous stress tensor.

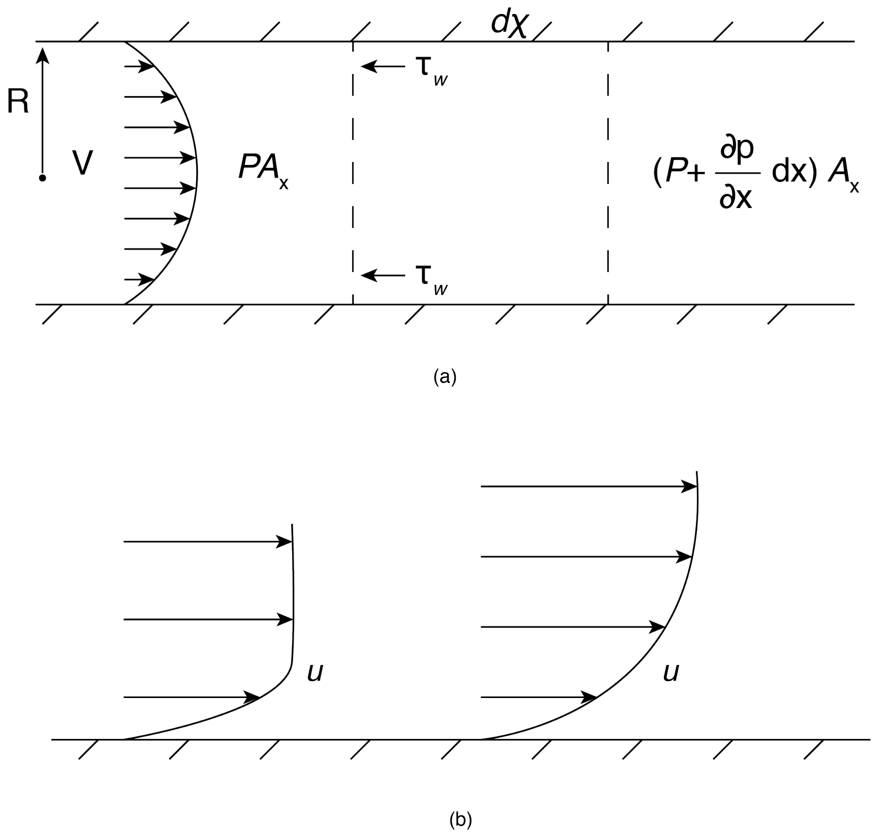

Fig 7.1 Illustration of velocity profiles (a) steady fully developed pipe flow resulting in a balance of pressure forces and wall friction forces, (b) external flow over a flat surface indicating boundary layer profile.

Viscous Stress

Viscous forces are represented here using the viscous stress tensor, τ_{ij}, that contains nine possible elements in three-dimensional space, three diagonal elements, i=j, and six off diagonal terms. Each of these terms will be given an interpretation relative to the flow. Physically the viscous stress is linked to the velocity gradient that results in a strain rate acting on a fluid element. Recall that fluids can have a continuous deformation with an applied force, in contrast to a solid which may have a given deformation proportional to the applied stress. We anticipate a relationship between the stress and the resultant strain rate occurring in the fluid. So first we define the strain rate that occurs within the fluid.

A small fluid element is shown in Fig. 7.2. First consider Fig. 7.2 (a) showing a "linear strain". Assume there exists an increase of u_1 in the x_1 direction, $\dfrac{\partial u_1}{\partial x_1} dx_1$, as a result, the surface of the element on the right (at larger x_1) will move faster to the right than the surface on the left (at smaller x_1). Over time Δt the distance between the two surfaces, denoted as "l" which is originally dx_1 will increase by Δl leading to a rate change of separation distance, or a rate of deformation equal to:

$$\frac{1}{l}\left(\frac{\triangle\, l}{\triangle\, t}\right) = \frac{\triangle\, l/l}{\triangle\, t} = \frac{\partial u_1}{\partial x_1} \tag{7.2}$$

Treating $\Delta l/l$ as the strain then Eqn. (7.2) represents the linear strain rate in the x_1 direction caused by the u_1 velocity gradient in the x_1 direction. We can write similar expressions for the x_2 and x_3 directions as $\frac{\partial u_2}{\partial x_2}$ and $\frac{\partial u_3}{\partial x_3}$, respectively. Physically, for positive values of these velocity gradient components in each direction we see that there is a stretching in each direction, there is similar compression if the derivatives are negative. There is a change of volume per time of $\frac{(\triangle\, l/l)_1}{\triangle\, t}(\partial x_1 \partial x_2 \partial x_3) = \frac{\partial u_1}{\partial x_1}(\partial x_1 \partial x_2 \partial x_3)$. Similarly in all 3 directions. Taken together over time there is a change in volume of the fluid element measured by the sum of the total change in each direction. Dividing through by volume $(\partial x_1 \partial x_2 \partial x_3)$ we call this result the "dilation rate" of the fluid. Using tensor notation we can write the dilation rate (using the summation rule) as:

$$\frac{\partial u_i}{\partial x_i} = \dot{e}_{ii} \tag{7.3}$$

(Where summation is implied)

The units of $\dot{e}_{ii}$ are one over time.

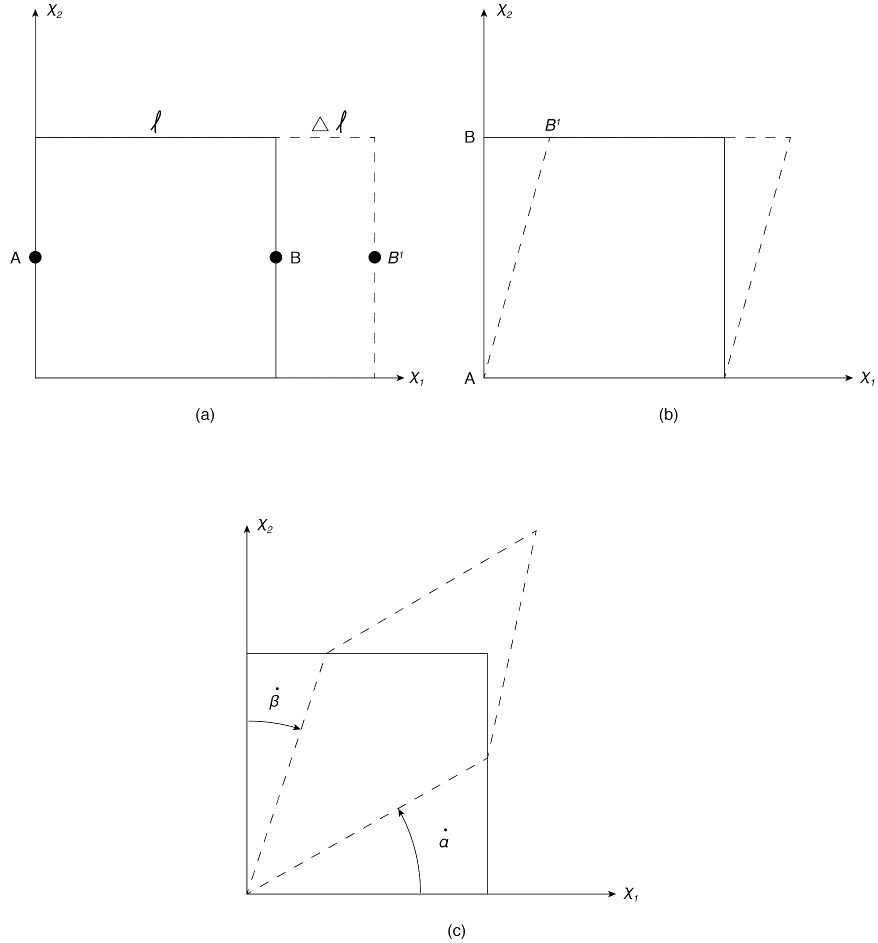

Fig 7.2 Strain rate deformation showing both (a) linear deformation rates and (b) angular deformation rates; in (c) the net angular deformation rate is zero when $\dot{\alpha} = \dot{\beta}$.

Now consider Fig. 7.2 (b), which shows the shear strain rate. Or the rate of strain caused by a shearing force. In this case two points on the element surface, A and B, will have a change of orientation relative to a fixed coordinate system. So points A-B will move to A-B' if the x_1 component of velocity increases in the x_2 direction. As shown this can be interpreted as a rotation of the line connecting A-B. If distance B-B' is length Δl and the line length A-B = $dx_2 = l$ then:

$$\frac{\Delta l / l}{\Delta t} = \frac{\partial u_1}{\partial x_2} \tag{7.4}$$

We can interpret this as a rotation, or angular strain rate, which in this case is about the x_3 axis. Similarly there can be a rotation about x_3 caused by rate, $\dfrac{\partial u_2}{\partial x_1}$. This can be repeated to obtain angular strain rates about each of the other axes as well.

These results provide the basis for the definition of the strain rate tensor, $\dot{e}_{ij}$:

$$\dot{e}_{ij} = \frac{1}{2}\left(\frac{\partial u_i}{\partial x_j} + \frac{\partial u_j}{\partial x_i}\right) \tag{7.5}$$

Notice that when i=j the strain rate tensor consists of components of the dilation rate, for instance $\frac{\partial u_1}{\partial x_1}$, etc. When $i \neq j$ we see the addition of the two terms causing rotation about any given axis. For instance if i=1 and j=2 we obtain rotation about the x_3 axis as shown above. But also, if i=2 and j=1 we also obtain rotation about the x_3 axis. In fact when added to calculate $\dot{e}_{ij}$ these resultant two cases are identical in value. This implies that the strain rate tensor is symmetric, $\dot{e}_{ij} = \dot{e}_{ji}$. Keep in mind that when the velocity derivative component is negative we have rotation in the opposite direction. The sign convention is that counter-clockwise rotation is positive. The inclusion of ½ is a matter of convenience as we will see later, but also can be thought of as providing an average of the two terms.

The general strain rate tensor, $\dot{e}_{ij}$, consists of all possible combinations of velocity spatial derivatives, and contains 9 elements. The diagonal terms are "linear deformation rates" and the off diagonal terms are the "shearing deformation rates". Notice that there are really only six definitive terms, since this is a symmetric tensor.

Recall that vorticity, is a measure of rotation rate as well. We need to distinguish this from the strain rate tensor. Consider the case of ω_3:

$$\omega_3 = \left(\frac{\partial u_2}{\partial x_1} - \frac{\partial u_1}{\partial x_2}\right) \tag{7.6}$$

First we notice the sign difference for the second term in the parenthesis when compared with the strain rate tensor. What is the consequence of this? If rotation caused by $\frac{\partial u_2}{\partial x_1}$ is counter clockwise because this derivative is positive, and the rotation caused by $\frac{\partial u_1}{\partial x_2}$ is negative when this derivative value is positive, then applying this to the above definition of ω_3 results in a net positive rotation (counter clockwise) about the x_3 axis. Or said another way, the vorticity is the sum of the two contributions of positive rotation rate about a given axis. Notice that vorticity has only three terms needed to define it (hence it is a vector). The diagonal terms are identically zero and the off diagonal terms are just of opposite sign (an antisymmetric tensor).

It is then possible to have zero vorticity (the two terms in the vorticity definition cancel) but still have a positive angular deformation. Consider the case of $\frac{\partial u_2}{\partial x_1} = \frac{\partial u_1}{\partial x_2}$ where the rotation rate is zero but the net angular deformation rate is not, and equal to twice the value of each component. This addition is shown schematically for a fluid element in Fig. 7.2 (c) where the net rotation about the x_3 axis would be zero if $\dot{\alpha} = \dot{\beta}$, but we see deformation of the fluid element.

We do one last manipulation. Suppose we identify the velocity gradient tensor as $\dfrac{\partial u_i}{\partial x_j}$. This has nine elements of all of the partial derivatives of the three components in the three coordinate directions. This second order tensor can be written as:

$$\frac{\partial u_i}{\partial x_j} = \frac{1}{2}\left(\frac{\partial u_i}{\partial x_j} + \frac{\partial u_j}{\partial x_i}\right) + \frac{1}{2}\left(\frac{\partial u_i}{\partial x_j} - \frac{\partial u_j}{\partial x_i}\right) \tag{7.7}$$

The first term on the right hand side is the deformation rate tensor and the second term is ½ of the vorticity, which (when including the ½) is identified as the rotation rate tensor. The latter can be thought of as the average rotation about any given axis. So the velocity gradient tensor consists of two parts, that due to the strain rate and that due to the vorticity (or rotation rate).

At this point we will construct a fairly simple model for the relationship between viscous stress and deformation rate to be as follows:

$$\tau_{ij} \sim \dot{e}_{ij}$$

This implies that the rate of deformation that occurs in a fluid element is directly proportional to the stress applied to that element. If we make the assumption that there is a proportionality factor equal to 2 μ, then we can write this as:

$$\tau_{ij} = \mu\left(\frac{\partial u_i}{\partial x_j} + \frac{\partial u_j}{\partial x_i}\right) \tag{7.8}$$

It is obvious why the factor 2 was introduced. Notice that the relationship does not include any of the rotational components of the velocity gradient tensor, only the deformation rate components. The physical interpretation is that viscous stress is related to the degree of deformation occurring in a fluid element, not its rotation rate.

Looking at the normal stress components, when $i = j$, we see that these terms result in linear deformation. As noted above these are elongation or contraction rates of a fluid element as it flows over time. Adding all three dimensions we get the net volume change of the fluid element over time. Consequently, according to the model of Eqn. (7.8) the viscous forces resulting in normal viscous stress components are responsible for these linear deformation rates. These stresses are the normal, or diagonal, components of τ_{ij}.

The shearing contributions of τ_{ij} are the off diagonal terms and are related through Eqn. (7.8) to the off diagonal terms of the strain rate tensor, $\dot{e}_{ij}$. These terms result in an angular deformation rate that distorts the original shape of the fluid element over time. Again, according to eqn. (7.8) this angular deformation rate, due to shearing viscous stresses, has a magnitude determined by the parameter, μ.

The parameter μ is a fluid property and can take on many forms depending on the characteristics of the fluid itself. This property is the fluid dynamic viscosity and may be a function of the state of the fluid (say its pressure or temperature), but it may also be a function of the stresses applied to the fluid. A Newtonian fluid is one that can have state varying viscosity (say like an oil that has decreasing viscosity with increasing temperature) but has a constant value of viscosity with changing stress within the fluid. These fluids have a linear relationship between viscous stress and deformation rate.

A dilatant fluid is described as shear thickening. That is to say as a shearing stress is applied to the fluid the viscosity increases. This implies that increasing stresses will result in decreasing deformation rates, consequently not having a linear relationship. Mixtures of cornstarch and water can behave as a dilatant fluid. In contrast, a fluid with a decreasing viscosity with increasing applied stress is called pseudo-plastic, or shear thinning, fluids. Examples of this type of behavior is ketchup, some paints, ink, and others. Fig. 7.3 illustrates the stress-strain rate relationship for various types of fluids where the slope is a measure of viscosity. For the remainder of this book we will deal with Newtonian fluids. Keep in mind, however, functional relationships can be used for non-Newtonian fluid viscosities, whereas we will use constant values in the problems we examine.

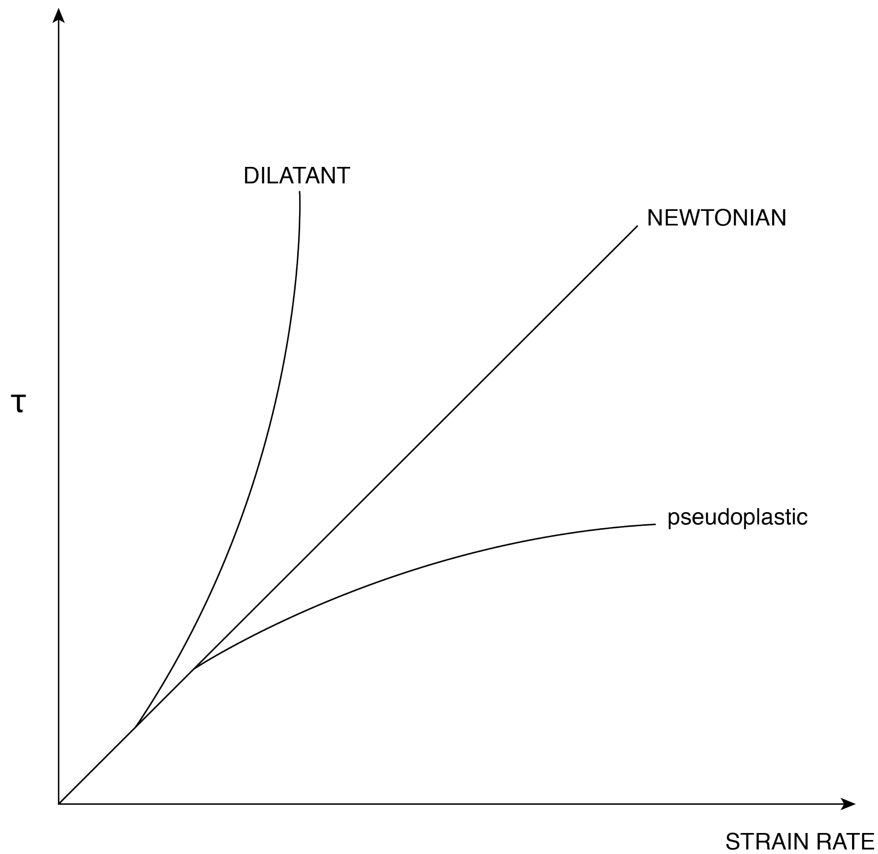

Fig 7.3 Illustration of the relationship between stress and strain rate for different fluids; shear thickening fluids have increasing viscosity (slope) with increasing stress (dilatant fluids) whereas shear thinning fluids have decreasing viscosity with increasing stress (pseudoplastics); Newtonian fluids have a constant viscosity with strain rate, or a linear relationship.

Navier-Stokes Equation

The Navier-Stokes equation is an extension of Euler's equation with the addition of the viscous forces. The Euler equation is written as:

$$\rho\frac{Du_i}{Dt} = \frac{\partial P}{\partial x_I} + \rho g_i$$

which is a balance of mass times acceleration per volume on the left hand side with the net force due to pressure gradients and the gravitational body force, both per volume of fluid. It should be noted that if we combine the pressure terms with the viscous stress terms we obtain the combined total stress expression:

$$\sigma_{ij} = -P\delta_{ij} + \tau_{ij} \tag{7.9}$$

We use the Kronecker delta, δ_{ij}, which is equal to one when i=j and otherwise equal to zero. This conveniently indicates that P is a normal compressive stress component. The negative sign indicates that pressure is compressive.

An additional force is introduced to account for forces that result in volume changes of a given fluid element. This is modeled as follows. As noted above the rate change of fluid volume per original volume is given by $\frac{\partial u_k}{\partial x_k}$, where there is summation over index k. Assuming that the force required to change the volume is a compressive normal force, and proportional to the volume change, we can write this force as:

$$\lambda \frac{\partial u_k}{\partial x_k} \delta_{ij}$$

where λ is a proportionality constant dependent on the fluid. This is added to the above stress expression to yield:

$$\sigma_{ij} = -P\delta_{ij} + \tau_{ij} + \lambda \frac{\partial u_k}{\partial x_k} \delta_{ij} \tag{7.10}$$

The net force per volume of fluid due to the stress can be written as:

$$\frac{\partial \sigma_{ij}}{\partial x_j} \tag{7.11}$$

Recall that there is a summation over the index *j* indicating that this expression is in a vector in the *i* direction. Inserting Eqn. (7.8) for the stress term in Eqn. (7.10), and then insert this result into Eqn. (7.11) results in the net stress force on a fluid element. This is then added to the Euler equation keeping in mind that we have already included the pressure term with the stresses. The result is:

$$\rho \frac{Du_i}{Dt} = \frac{\partial \sigma_{ij}}{\partial x_j} + \rho g_i = -\frac{\partial P}{\partial x_j} \delta_{ij} + \frac{\partial}{\partial x_j} \left(\lambda \frac{\partial u_k}{\partial x_k} \right) \delta_{ij} + \rho g_i + \frac{\partial}{\partial x_j} \left(\mu \left(\frac{\partial u_i}{\partial x_j} + \frac{\partial u_j}{\partial x_i} \right) \right) \tag{7.12}$$

This equation has three velocity components and the pressure as unknowns. Two fluid parameters, μ and λ are also included. The parameter λ is known as the coefficient of bulk viscosity, and is representative of the force required to change the fluid volume.

For an incompressible fluid, since $\frac{\partial u_k}{\partial x_k} = 0$, (with summation) this term disappears.

For a compressible fluid Stokes hypothesis is that:

$$\lambda = -\frac{2}{3} \mu \tag{7.13}$$

This comes with some theoretical justification and has been shown over a wide range of conditions to be reasonably valid, but shown not to be valid for extreme pressures. Since in this book we restrict ourselves to incompressible flows, this is not an issue and we will neglect this term. Also, for incompressible flows with constant viscosity we can simplify the last (viscous) term in Eqn. (7.12) as:

$$\frac{\partial}{\partial x_j}\left(\mu\left(\frac{\partial u_i}{\partial x_j}+\frac{\partial u_j}{\partial x_i}\right)\right)=\mu\frac{\partial^2 u_i}{\partial {x_j}^2}+\mu\left(\frac{\partial}{\partial x_i}\left(\mu\frac{\partial u_j}{\partial x_j}\right)\right)=\mu\frac{\partial^2 u_i}{\partial {x_j}^2} \tag{7.14}$$

wherein the second term in the middle expression we have reversed the order of differentiation of x_i and x_j and then invoked the incompressible condition leaving only the first term, which is the Laplace of the velocity vector.

The final form of the Navier-Stokes equation that we will use for incompressible constant viscosity (Newtonian fluid) flows is:

$$\rho\frac{Du_i}{Dt}=\rho\frac{\partial u_i}{\partial t}+\rho u_j\frac{\partial u_i}{\partial x_j}=-\frac{\partial P}{\partial x_j}\delta_{ij}+\rho g_i+\mu\frac{\partial^2 u_i}{\partial {x_j}^2} \tag{7.15}$$

The left hand side has been expanded to show the local and convective acceleration terms and on the right hand side we have force contributions from pressure gradients, gravity and viscous forces (normal and shearing). This equation is coupled with the requirements for incompressible flow:

$$\frac{\partial u_k}{\partial x_k}=0 \tag{7.16}$$

Notice, since we have incompressible flow it is possible to rewrite the convective acceleration term:

$$\rho u_j\frac{\partial u_i}{\partial x_j}=\rho\frac{\partial\left(u_i u_j\right)}{\partial x_j} \tag{7.17}$$

Sometimes this may be referred to as the "conservative form" of the Navier-Stokes equation since it takes advantage of the conservation of mass for incompressible flow.

We can also rewrite the Navier-Stokes equation using the definition of vorticity. First the convective acceleration term invokes the vector identity mentioned, in an earlier chapter in discussion of the generalized Bernoulli equation, that is written as:

$$\rho u_j\frac{\partial u_i}{\partial x_j}\ =\ \rho\left(\frac{\partial\left(\frac{1}{2}u_j u_j\right)}{\partial x_i}+\varepsilon_{ijk}\omega_j u_k\right) \tag{7.18}$$

The viscous terms can also use the following vector identity:

$$\mu \frac{\partial^2 u_i}{\partial {x_j}^2} = -\mu \varepsilon_{ijk} \frac{\partial \omega_k}{\partial x_j} \tag{7.19}$$

This last term is the viscosity times the curl of the vorticity. Notice what happens when the flow is irrotational. The second term of Eqn. (7.18) is zero and the viscous stress term, Eqn. (7.19), is also zero. It is left for the reader to see that under these conditions one can arrive at the simplified Bernoulli equation when integrated between any two points within the flow field. If the flow is inviscid the last term of Eqn. (7.15) is zero, but the flow is not necessarily irrotational since the vorticity also enters into the equation in the convective acceleration term. So, an irrotational flow does imply an inviscid flow but an inviscid flow does not imply irrotational flow. Lastly, the viscous term vanishes if the curl of the vorticity is zero, it is not necessary that the flow be irrotational.

Examples of Exact Solutions to Navier-Stokes Equation

Steady Flow Between Parallel Plates or in a Circular Pipe

For fully developed, steady flow between parallel plates shown in Fig. 7.4 using Cartesian coordinates with flow in the x_1 direction the reader should verify that there is no acceleration and the Navier-Stokes equation reduces to a balance of forces. If the flow is horizontal there is only pressure and viscous forces that balance. If the flow is vertical with no pressure driving the flow then there is a balance of gravitational forces and viscous forces. For plates with a separation distance of 2h with the x_1 axis along the centerline between the plates, as shown in the figure, the form of the velocity distribution in both cases is identical. Note that since there is only the u_1 velocity component then $\frac{\partial u_1}{\partial x_1} = 0$ and we say the flow is fully developed, with no changes in the flow direction and no convective acceleration. For steady flow there is no local acceleration.

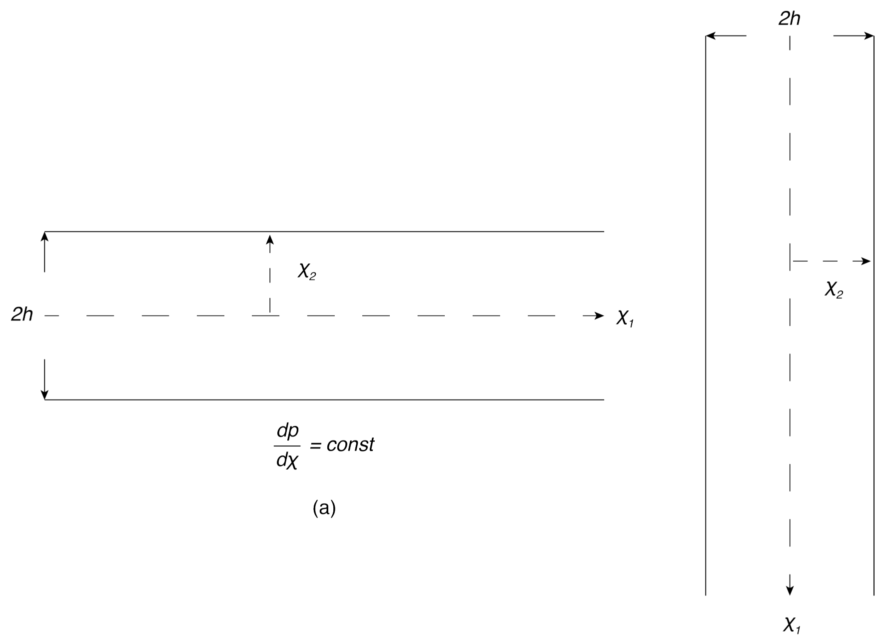

Fig 7.4 Illustration of steady flow between parallel plates, left is a constant pressure gradient driven flow and on the right is a gravity driven flow; the x_1 coordinate is in the flow direction and x_2 is normal to the flow.

Consider horizontal flow, so no body force, to determine the velocity distribution we first examine the pressure gradient term for this case. Since there is no acceleration the pressure term is balanced by the viscous terms. The resulting Navier-Stokes equation is:

$$0 = -\frac{\partial P}{\partial x_j}\delta_{ij} + \mu\frac{\partial^2 u_i}{\partial {x_j}^2} = \frac{dP}{dx_1} + \mu\frac{d^2 u_1}{dx_2^2}$$

To explain why we can write the terms as ordinary derivatives consider the following. Since the acceleration is zero we can say that $u_1 \neq f(x_1)$ which is also found from the conservation of mass noting that $u_2 = u_3 = 0$. Based on this we can say that the viscous term is not a function of x_1, so therefor the pressure term is not a function of x_1 either. At most u_1 is a function of x_2. One can show that dP/dx_1 is not a function of x_2 from the x_2 momentum equation. So if the change of P along the flow is not a function of x_2 or x_1, then dP/dx_1 is a constant.

By applying the no-slip boundary condition at the wall surfaces, x_2 = +/- h the result is:

$$u_1 = C\left(1 - \frac{{x_2}^2}{h^2}\right) \tag{7.20}$$

where $C = -\dfrac{h^2}{2\mu}\dfrac{dP}{dx_1}$ for pressure driven horizontal flow and $C = \dfrac{\rho g h^2}{2\mu}$ for gravity driven vertical downward flow.

Given this velocity field the vorticity distribution can be determined and since the velocity is parabolic the vorticity distribution will be piecewise linear across the flow with zero value at the center, and maximum value at the surface, $\omega_3 = -\dfrac{2C}{h^2}x_2$.

The same flow can be considered for flow in a round constant area horizontal pipe. This is often called Hagen-Poiseuille flow after two experimentalists who developed this relationship in the 1800s for steady pipe flow in the form of flow rate versus pressure drop. In this case the Navier-Stokes equation is written in cylindrical coordinates as shown in Table 7.1 and then reduced for steady, constant area, incompressible, constant property flow. Again, the flow has no acceleration for steady, constant area flow and the result is a balance of pressure and viscous forces in the z, or axial direction. The pressure gradient along z is a constant similar to the result for flow between parallel plates. The resulting simplified equation is integrated across the flow (r coordinate) using the no-slip boundary condition at $r = R$ (R is the pipe radius) and also noting that the velocity is a maximum at the centerline where the velocity derivative in r is zero. The result is:

$$v_z = -\frac{R^2}{4\mu}\frac{dP}{dz}\left(1 - \frac{r^2}{R^2}\right) \tag{7.21}$$

For all of these internal flows the flow rate can be obtained by integrating the velocity distribution across the flow area. For instance, for a volumetric flow rate of $\dot{Q}$ and writing the pressure gradient $(-dP/dx_1)$ as $\Delta P/L$ since it is constant (notice the sign change since ΔP is the upstream pressure minus the downstream pressure) and L is the total length along x_1. We have for steady horizontal pressure driven flow between parallel plates:

$$\dot{Q} = \frac{2h^3\Delta P}{3\mu L} l \text{ (per distance } x_3\text{)} \tag{7.22}$$

For steady flow in a pipe:

$$\dot{Q} = \frac{\pi R^4 \Delta P}{8\mu L} \tag{7.23}$$

It is straight forward to evaluate similar relationships for gravity driven flows by replacing the pressure gradient with ρg.

There are a number of other steady flows that can also be solved for analytically from the Navier-Stokes equation. For instance, steady axial flow in an annulus, either pressure or gravity driven; flow in the gap between two rotating cylinders that have different rotation rates; flow between parallel plates where one plate is moving relative to the other with or without a pressure gradient or gravity driving the flow, and a few others. All of these flows have no local or convective acceleration terms and the basic governing equation is a balance of forces. It is possible to solve some flows with acceleration as shown next.

Suddenly Accelerated Plate (Stokes First Problem, also known as the Rayleigh Problem)

When a flat plate is immersed in a large body of fluid, and the plate is suddenly accelerated to some fixed, constant velocity the fluid surrounding the plate will be set into motion. This general problem is known as Stokes first problems, named for Sir George Stokes the well-known mathematician, for whom the Navier-Stokes equation is also named. There are variations on this problem, such as the flow field set up in a fluid when the plate oscillates back and forth sinusoidally, Stokes second problem. Here we will look at the solution one can obtain for the first problem. It will introduce the idea of a similarity formulation of the problem and provide insight on how to nondimensionalize results. It is also useful in the interpretation of boundary layer flows that we will examine in a later chapter.

This is an idealized problem where the plate is assumed to accelerate instantaneously to some velocity $U = U_p$ and remains at that velocity. Obviously there is some finite time for this to happen, but we ignore that (short) time effect. Fig. 7.5 illustrates the coordinate system and the flow. By symmetry we only need to include one half of the flow field, on top, and we assume that the plate is infinite in extent in the x_1, x_3 directions. The flow is only in the x_1 direction, to the right. There are no forcing functions is the x_2 and x_3 directions so we take u_2 and u_3 to be zero. Finally the fluid is assumed to extend infinitely far in the +/- x_2 directions.

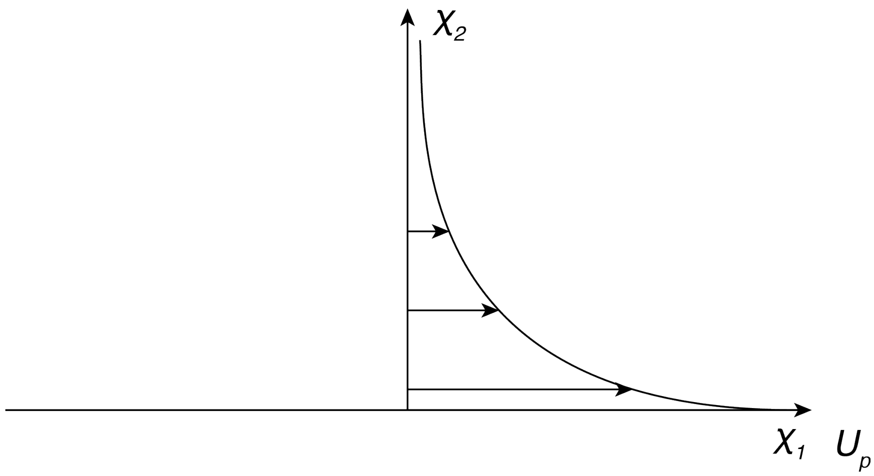

Fig 7.5 Velocity profile associated with a horizontal plate with near instantaneous acceleration to a constant velocity of U_p at time zero; fluid above the plate is set into motion by viscous forces; the extend of the flow domain above the plate increases with time.

This problem may model the start up of a plate with lubricating oil between the plate and some surrounding surfaces, at least for early times before the flow is influenced by the surrounding surfaces (we will be able to determine this time from our solution).

The analysis begins using the x_1 direction Navier-Stokes equation and eliminating all zero valued terms. Assuming the flow is governing by viscous forces between the surface and fluid, and neglecting any establish pressure variation within the flow we have the simplified form:

$$\frac{\partial u_1}{\partial t} = \nu \frac{\partial^2 u_1}{\partial x^2} \tag{7.24}$$

where $\nu = \mu/\rho$ which is called the kinematic viscosity and has SI units of $(m^2$/s). This is obtained by dividing through by the fluid density. The associated boundary and initial conditions are:

No-slip: $u_1 = U_p \; at \; x_2 = 0$

No flow far from the surface: $u_1 = 0 \; at \; x_2 \rightarrow \infty$

Initially no flow: $u_1 = 0 \; at \; t = 0 \; for \; all \; x_2$

This is what is called a "diffusion" problem where velocity (or momentum per mass) of the fluid diffuses away from a source of momentum (the wall friction force). Fick's law of diffusion states that the diffusion rate, or flux of a quantity, is proportional to the local gradient of the quantity. As we will see this diffusion process is directly linked to the fluid viscosity.

The above governing equation can be scaled in several different ways. First let's use dimensional analysis with the condition that the velocity at any point in space and time within the fluid near the plate is a function of the following list of variables

$$u = (U_p, x_2,\ t,\ \nu) \tag{7.25}$$

where we have used u instead of u_1 since there is only one velocity component to consider. This list of variables should be obvious from the governing equation, (7.24) and the associated initial and boundary conditions. Now using dimensional analysis we arrive at the following three nondimensional Pi groups:

$$\Pi_1 = \frac{u}{U_p}, \Pi_2 = \frac{x_2}{\sqrt{\nu t}}, \Pi_3 = \frac{x_2}{U_p t} \tag{7.26}$$

However, Π_3 provides no new information since all of the variables appear in the other two Pi groups. Hence we can conclude that

$$\Pi_1 = f\left(\Pi_2\right) \text{ or } \frac{u}{U_p} = f\frac{x_2}{\sqrt{\nu t}} \tag{7.27}$$

This implies that the velocity scaling for this problem is U_p and the length scale is $\sqrt{\nu t}$. Notice here that the length scale is a function of time. That is to say that the extent of the length scale increases over time, and is not a constant. We can think of this length scale as roughly the distance over which diffusion is expected to occur, which is time dependent. For convenience in the mathematics we will add an arbitrary "2" to the length scale and express it as:

$$\frac{u}{U_p} = f(\frac{x_2}{2\sqrt{\nu t}}) \tag{7.28}$$

We have two variables, $f = \dfrac{u}{U_p}$ and $\eta = \dfrac{x_2}{2\sqrt{\nu t}}$. And we seek a solution of $f(\eta)$. The next step is to substitute our nondimensional variables into the governing equation and initial and boundary conditions. This needs to be done carefully since one of our scales (length) is a function of time. The reader is encouraged to go through the following transformation using the chain rule:

$$\frac{\partial u}{\partial t} = \frac{\partial (f U_p)}{\partial \eta} \cdot \frac{\partial \eta}{\partial t} = U_p \frac{\partial f}{\partial \eta}(-\frac{\eta}{2t})$$

$$\frac{\partial u}{\partial x_2} = U_p \frac{\partial f}{\partial \eta} \cdot \frac{\partial \eta}{\partial x_2} = U_p \frac{\partial f}{\partial \eta} \frac{1}{2\sqrt{\nu t}}$$

$$\frac{\partial^2 u}{\partial {x_2}^2} = \frac{\partial}{\partial x_2}\left(U_p \frac{\partial f}{\partial \eta} \cdot \frac{\partial \eta}{\partial x_2}\right) = U_p \frac{\partial f}{\partial \eta} \frac{\partial^2 \eta}{\partial {x_2}^2} + U_p \frac{\partial \eta}{\partial x_2} \frac{\partial^2 f}{\partial \eta^2} \frac{\partial \eta}{\partial x_2}$$

$$\frac{\partial^2 u}{\partial {x_2}^2} = U_p \left(\frac{1}{2\sqrt{\nu t}}\right)^2 \frac{\partial^2 f}{\partial \eta^2}$$

Inserting the first and the last of this set of equations in Eqn. (7.24) the result is:

$$\frac{\partial^2 f}{\partial \eta^2} + 2\eta \frac{\partial f}{\partial \eta} = 0 = f'' + 2\eta f' \tag{7.29}$$

where the last expression is used to write derivatives as primes (f'' is the second derivative and f' is the first derivative.) Notice here that the derivatives can actually be ordinary derivatives since as shown in (7.27) f is only a function of η. Importantly here the second order partial differential equation in two variables is transformed into a second order ordinary differential equation, which in general has a much easier solution.

The next step is to transform the boundary conditions as follows:

$$\text{at } \; x_2 = 0 \;\; \eta = 0 \text{ and } u = U_p \text{ so } f(0) = 1 \tag{7.30}$$

$$\text{as } x_2 \to \infty \quad \eta \to \infty \text{ and } u \to 0 \text{ so } \; f(0) = 0$$

$$\text{at } t = 0 \quad \eta \to \infty \; \text{ and } u \to 0 \text{ so } \; f(0) = 0$$

The last two conditions are identical, so we end up with two boundary conditions for η which is what we expect since we have a second order equation. We are left with the governing equation (7.29) and the boundary conditions (7.30). It turns out that there is an analytical solution. Letting:

$$g = f'$$

then the governing equation is:

$$\frac{g'}{g} = -2\eta$$

this can be integrated to:

$$g = f' = C_1 e^{-\eta^2}$$

which we integrate again to:

$$f = C_1 \int_0^\eta e^{-\eta^2} d\eta + C_2 \tag{7.31}$$

The first term on the right hand side is a straightforward integral evaluation up to a variable value η. This can be replaced by the Gaussian Error Function, $erf(\eta)$ which is shown in Fig (7.6) as:

$$erf\,(\eta) \;= \frac{2}{\sqrt{\pi}} \int_0^{\eta} e^{-\eta^2}\, d\eta$$

so that:

$$f = \frac{\sqrt{\pi}}{2} C_1 erf\,(\eta) \;\; + C_2$$

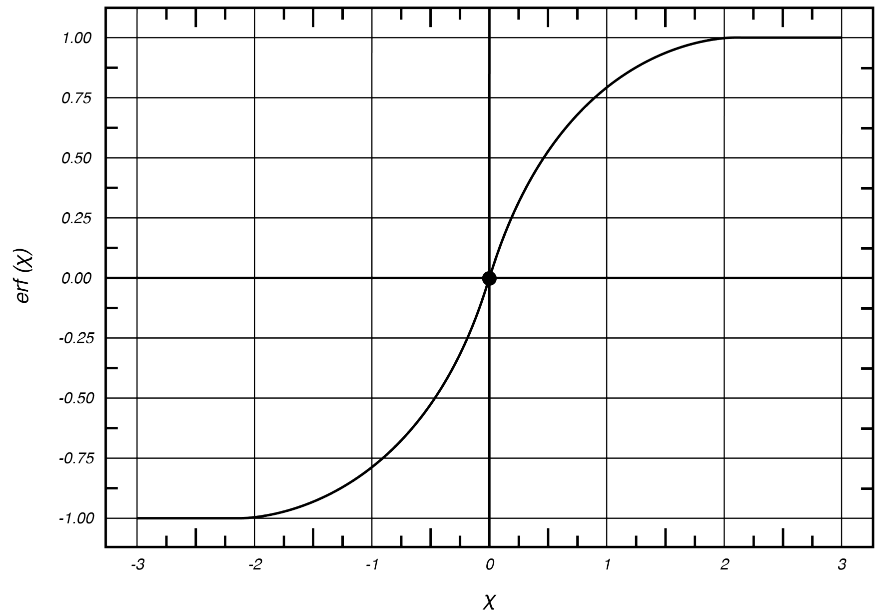

Fig 7.6 Gaussian Error Function, erf(x), where x is the argument; the function is normalized to vary between -1 and +1 and passes through zero at $x = 0$.

We are left to evaluate the constants from the two boundary conditions for *f*.

Since $erf(0) = 0$ and $erf(\infty) = 1$ then $C_1 = -\frac{2}{\sqrt{\pi}}$ and $C_2 = 1$ and the final form of the equation is:

$$f = \frac{u}{U} = 1 - erf(\eta) \text{ and } f' = -\frac{2}{\sqrt{\pi}} e^{-\eta^2} \tag{7.32}$$

The results of Eqn. (7.32) are plotted in Fig. 7.7. This solution is a "similarity solution" in that the results collapse, in this case, into a single variable, η, which depends on the two independent variables, x_2 and

t. There are two parameters affecting the result of the local velocity, the boundary condition, U_p, and the fluid property, ν. To evaluate a given set of conditions one does the following. (1) Identify the physical space and boundary conditions of interest. (2) Transform variables such as values of space or time into associated values of the variable η. (3) Use Eqn. (7.32) to determine the value of f versus η and the desired η value. (4) Transform f into the desired velocity u.

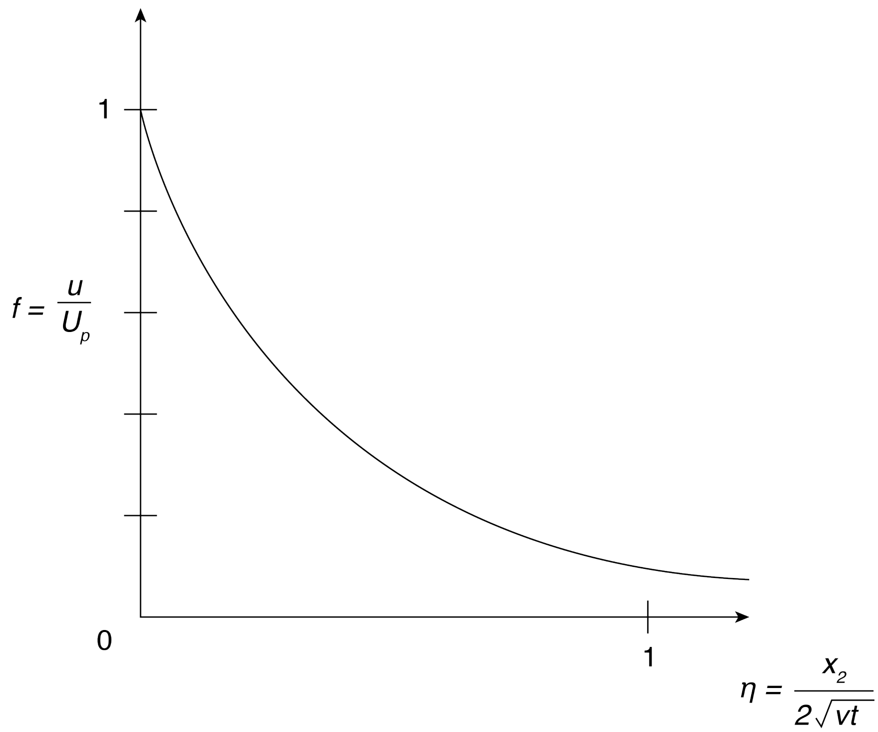

Fig 7.7 Nondimensional result of f' versus η.

Besides determining the local velocity in the fluid these results are also useful in determining the transient wall shear stress, or force per unit area of the plate. Given in Eqn. (7.32) is the derivative, f'. This provides information of the velocity derivative, $\dfrac{\partial u}{\partial x_2}$. Since there is only one velocity component and it is only a function of x_2 we can write the shear stress as:

$$\tau = \mu\left(\frac{\partial u_2}{\partial x_1} + \frac{\partial u_1}{\partial x_2}\right) = \mu\frac{\partial u_1}{\partial x_2} = \mu\left(\frac{Uf'}{2\sqrt{\nu t}}\right) \tag{7.33}$$

where f' is the derivative $\dfrac{\partial f}{\partial \eta}$. The force on the surface of the plate with an area of LS, (where L is the distance along the plate in the direction of motion and S is the width, or span of the plate) due to its motion is:

$$F_p = \int_0^L \tau_s dx_1 S \tag{7.34}$$

where the shear stress, τ_s, is evaluated at the surface where x_2 = 0. Evaluating (7.34) using (7.33) at $\eta = 0$, with $f'(0) = -\dfrac{2}{\sqrt{\pi}}$ results in:

$$\tau_s = -\frac{\mu U_p}{\sqrt{\pi \nu t}}$$

and the force

$$F_p = -\frac{\mu U_p L S}{\sqrt{\pi \nu t}} \tag{7.35}$$

Notice that the wall stress decreases with time as momentum diffuses away from the surface. The force therefore also decreases with time. At time t = 0 the equations have a problem, since we said the acceleration was initially infinite.

We can define the diffusion distance way from the surface as the distance x_2 to where the velocity decays to 1% (small arbitrary value) of the plate velocity. So setting f = 0.01 we see that η = 1.85 and setting $x_2 = \delta$ at this point we have:

$$\delta = 3.7\sqrt{\nu t} \tag{7.36}$$

Notice that the diffusion distance increases with time as well as kinematic viscosity. The greater the viscosity the further is the distance, δ, at any given time. It is independent of the plate velocity.

One last item on this seemingly simple problem that will help in the interpretation of boundary layer flows. This flow has vorticity, but only aligned with the x_3 direction, as can be seen by calculating the local vorticity distribution:

$$\omega_3 = \left(-\frac{\partial u}{\partial x_2}\right) = -\frac{U f'}{2\sqrt{\nu t}} \tag{7.37}$$

The circulation is the area integral of the vorticity, so extending an integration from the surface at $x_2 = 0$ to δ, for a distance L along x_1, then the total circulation per distance x_3 becomes:

$$\Gamma = \int_0^\delta -\frac{U_p f'}{2\sqrt{\nu t}} dx_2 L = \int_0^\infty -U_p f' d\eta L = -U_p L$$

where for x_2 greater than δ the value of f' = 0 so there is no contribution to Γ.

Interestingly, the total circulation remains constant overtime, but the area grows since δ increases with time. The diffusion process merely spreads the vorticity over an increasing area, for increasing time and all of the vorticity is generated with the initial acceleration of the surface.

VIII. BOUNDARY LAYER FLOWS

In this chapter, we discuss the physical attributes associated with boundary layer flows. The governing equations are developed from the Navier-Stokes equation. The laminar boundary layer flow characteristics and interpretation of the associated forces generated by the flow are presented and discussed. This flow is a viscous dominated flow, rather than a pressure dominated flow. We will not explore the details associated with boundary layers on curved surfaces or surfaces that have flows influenced by an existing pressure gradient. Some physical insight into these conditions will be presented, however, and the concept of flow separation is introduced.

The pioneering work of Ludwig Prandtl soon after the beginning of the 20th century lays most of the groundwork for boundary layer analysis. His work has lead to an entire field of study that allows a combination of viscous dominated flows with inviscid flows. Prandtl used a very detailed combination of experimental and analytical methods to approach a very complex problem — the influence of fluid friction on streamline flows. He was very interested in wing theory and how to model real wing flows and their associated forces of lift and drag. The concept of a thin airfoil theory was developed and applied to three-dimensional wings. Here we will look at the basic physics associated with boundary layer theory and how these flows can be modeled for the laminar flow conditions. Turbulent flows are introduced in a later chapter.

Physical Attributes of a Boundary Layer

A boundary layer flow is defined to be the region of a larger flow field that is next to the surface and has significant effects of wall frictional forces. Since the region of interest is near the surface and the surface is assumed to be impervious to the flow then the velocity is nearly parallel to the surface. The general flow is shown in Fig. 8.1. Flow is from left to right and there is an upstream “leading edge” where the surface begins. At the leading edge (defined as the coordinate system origin), the flow immediately next to the surface begins to experience frictional forces due to the no slip boundary condition.

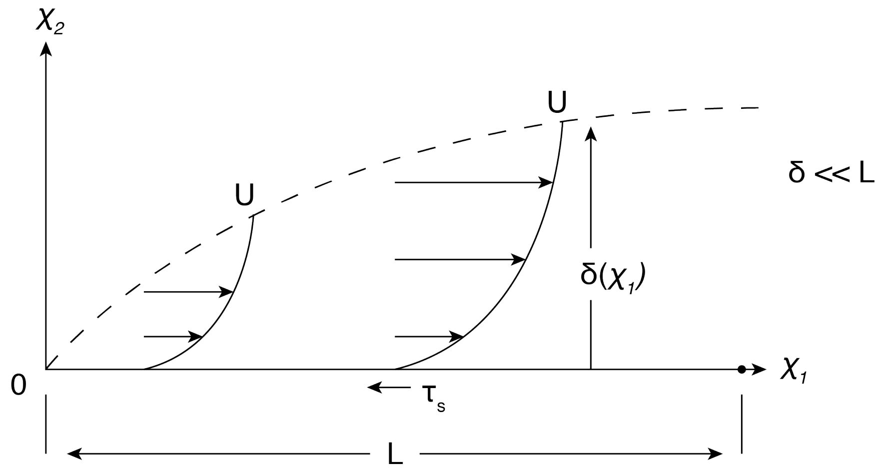

Fig 8.1 Illustration of boundary layer flower characteristics and coordinate system.

The fluid outside of this thin layer is directly unaffected by the wall friction. As the flow goes downstream the slower moving fluid near the surface exerts frictional forces on the fluid further away from the surface. This process is one of diffusion of momentum loss in a direction normal to the surface that results in a reduction of the local fluid velocity. The rate of diffusion depends on the viscosity of the fluid. As this happens the region slowed by friction grows such that the thickness of the boundary layer, δ, increases along the flow direction. At the outer edge of this viscous region, where the flow is no longer affected or slowed by the surface generated friction, the velocity is called the "freestream" value. The boundary layer flow shown in Fig. 8.1 represents a laminar flow condition where the boundary layer thickness extends further away from the surface at locations further along the flow direction. Turbulent flow has a similar trend but has some distinct differences in the velocity distribution and is discussed in a later chapter. Both laminar and turbulent flows must follow the no-slip boundary condition at the surface, resulting in zero relative velocity at the surface. The boundary layer thickness is affected by the turbulence and results in a thicker boundary layer in general.

Although we said that the flow is principally along the surface in the narrow boundary layer, there needs to also be a "wall-normal" velocity component, or u_2 using our coordinate system. The requirement of a non-zero velocity component away from the surface can be shown by using a control volume starting from the leading edge and extending downstream an arbitrary distance x_1 as shown in Fig. 8.2. Note that the control volume has the same area for flow inlet and outlet in the stream-wise direction, that is h is a constant. By applying conservation of mass to this control volume we obtain the following for steady flow:

$$0 = \dot{m}_3 + \dot{m}_2 - \dot{m}_1$$

where the subscripts refer to the different mass flows shown in Fig. 8.2, subscript 1 is the flow coming into the control volume from the left at the leading edge, subscript 2 is the flow going out the right side at distance x downstream and subscript 3 is flow that goes out the top. The flow coming in at the leading edge has a uniform velocity of U over the vertical distance h. The outflow at distance x_1 has been slowed by friction such that the velocity varies from zero at the surface to U at the outer edge of the boundary layer. Integrating this downstream velocity profile over the same vertical distance h will result in a lower mass flow rate than at the leading edge since $\dot{m}_2 < \dot{m}_1$. Consequently, $\dot{m}_3 > 0$ or, there must be a positive outflow, $\dot{m}_3$, resulting in a velocity component out the top of the control volume. The no-slip boundary condition requires that all velocity components are zero at the surface. This implies that the vertical velocity component must start at zero and increase with increasing x_2. Also, streamlines associated with the flow must deflect upwards along the flow direction to account for the nonzero x_2 velocity component, as is shown in Fig 8.2.

The characteristics of the developing velocity profile along the flow direction, x_1, can be used to understand the distribution of the surface shear stress τ_s. Since the boundary layer grows larger in the flow direction, as more and more of the fluid above the surface is slowed by friction, then at any given height, x_2, the velocity in the x_1 direction must decrease going in the x_1 direction. That is $\dfrac{\partial u_1}{\partial x_1} < 0$.

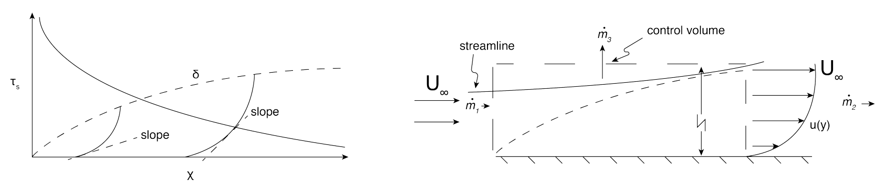

Fig 8.2 Distribution of the surface shear stress along the surface the shear stress continues to decreases as the boundary layer increases in the flow direction; control volume used to illustrate conservation of mass requirements for wall-normal flow.

The result of this is that the velocity distribution has a decreasing value of $\dfrac{\partial u_1}{\partial x_2}$ near the surface. That is to say, the velocity is always zero at the surface and always extends to U at the edge of the boundary layer, $x_2 = \delta$, so as δ increases the velocity derivatives $\dfrac{\partial u_1}{\partial x_2}$ everywhere within the flow must decrease. Based on this, the value of $\dfrac{\partial u_1}{\partial x_2}$ at the surface decreases in the x_1 direction. Using the definition of the shear stress and noting that $\dfrac{\partial u_1}{\partial x_1} = 0$ at the surface, we see that

$$\tau_s = \mu \left(\frac{\partial u_2}{\partial x_2} \right)_{x_2=0} \tag{8.1}$$

where the subscript $x_2 = 0$ means that it is evaluated at the surface. Since the surface velocity derivative decreases along x_1 then so does the surface shear stress and the qualitative result is the trend of τ_s shown in Fig. 8.2. Notice that the surface shear stress does not reach a constant value, as in pipe flow, since the flow never becomes fully developed, or $\dfrac{\partial u_1}{\partial x_1} \neq 0$.

If the surface is perfectly flat then the freestream flow outside the boundary layer will be nearly parallel with the surface (in the x_1 direction) at velocity U, except for the small upward velocity component described earlier. For parallel straight flow the change of pressure along the flow, and normal to the flow, is zero as we saw in inviscid flow. If we anticipate that the thickness, δ, of the boundary layer is relatively thin (we will show this to be the case later in this chapter when we develop the boundary layer equations) then the change of pressure due to hydrostatic effects between the outer edge of the boundary layer and the surface is small, even if the fluid is a liquid. However, even if hydrostatic pressure rise is not small across the boundary layer the change in pressure along the flow should in fact approach zero near the surface because the change in pressure along the flow is zero just outside of the boundary layer. This is explained by the following. The hydrostatic pressure change is the same between two vertical points evaluated at different locations along x_1. So the difference of pressure in the x_1 direction, $\dfrac{\partial P}{\partial x_1}$ will be identical for positions near the edge of the boundary layer and near the surface. So if $\dfrac{\partial P}{\partial x_1} = 0$ just outside the boundary layer then it is also zero inside the boundary layer. The net effect of this is that for a flat surface the pressure gradient along the flow is essentially zero. We will show this to be true based on the governing equations later in this chapter. We could extend this further for a curved surface and deduce that the pressure gradient for flow over the curved surface is the same outside and inside the boundary layer if the boundary layer is thin.

So a summary of the main attributes we will rely on for the analysis of boundary layers at this point are: (i) the boundary layer is thin, δ >> L, (ii), the wall normal velocity is small but finite, u_2 << u_1, (iii) for a (nearly) flat surface the pressure gradient is zero, $\partial P/\partial x_1 = 0$, (iv) the outer edge of the boundary layer velocity is the freestream velocity, U, which is determined by inviscid flow conditions.

Boundary Layer Equations

The boundary layer equations are a somewhat simplified form of the Navier-Stokes equations based on the physical attributes of the flow, listed above. The flow here is taken to be steady and two-dimensional, with velocity components in x_1 and x_2, which we designated by (u_1, u_2). Note that it is possible to have a more complex unsteady three dimensional version of boundary layer flow that is beyond the scope here. As part of the solution we will show that u_1 >> u_2. We assume the surface is perfectly flat and parallel to the oncoming fluid flow direction so there is no pressure gradient along the flow direction. Finally, we neglect any gravitational forces and assume we have incompressible flow. Strictly speaking the boundary layer equations do not require the pressure gradient to be zero, and can be treated as a parameter that allowed for some curvature of the surface (not flat).'

With the above conditions we write the x_1 direction Navier-Stokes equation as:

$$\rho\left(u_1\frac{\partial u_1}{\partial x_1}+u_2\frac{\partial u_1}{\partial x_2}\right)=\mu\left(\frac{\partial^2 u_1}{\partial {x_1}^2}+\frac{\partial^2 u_1}{\partial {x_2}^2}\right) \tag{8.2}$$

we combine this with the differential conservation of mass for an incompressible flow:

$$\left(\frac{\partial u_1}{\partial x_1}+\frac{\partial u_2}{\partial x_2}\right)=0 \tag{8.3}$$

At this point we have two-dimensional partial differential equations in two variables. It is worth noting here that the pressure gradient in the y direction, across the flow, is reduced to a very small number under the conditions that the u_2 component of velocity is very small compared with u_1, and that the boundary layer is thin so that there is essentially zero hydrostatic pressure variation across the flow. This can be shown by noting that all terms in the x_2 momentum equation containing u_2 become very small and the body force term is small since changes in x_2 are small, therefor the pressure gradient in x_2 must also be small. This process will become clearer in our discussions of scaling of the x_1 momentum equation below.

Next we scale the variables in the governing equation. This means coming up with appropriate scaling for each variable (dependent and independent) that is on the order of the maximum value of the variable. For instance, the characteristic length scale for flow over a flat plate with length L would be just L. Similarly, the characteristic velocity scale for the x_1 velocity component would be the freestream velocity, U. Below is listed the characteristic scales for the various variables (note that the scales may not be constant values as is noted by the choice of scale for x_2):

$$x_1 - L \tag{8.4}$$

$$x_2 - \ \delta$$

$$u_1 - U_\infty$$

$$u_2 - unknown$$

In general L can be any length of surface. We select δ to be the boundary layer thickness that coincides with this selected length in the analysis below. That is to say that the largest value of δ occurs at $x_1 = L$. But in general δ varies as we move in the x_1 direction. We do not know how large u_2 may be, but we can determine this by examining the conservation of mass, Eqn. (8.3). To do this we use the above scaling to form nondimensional variables, denoted by the superscript "*" by dividing each variable by its scale value:

$$x_1{}^* = \frac{x_1}{L} \tag{8.5}$$

$$x_2{}^* = \frac{x_2}{\delta}$$

$$u_1{}^* = \frac{u_1}{U}$$

$$u_2{}^* = \frac{u_2}{V_s}$$

where V_s is an unknown scale for variable u_2 and is to be determined. Inserting these non-dimensional variables into Equation (8.3), where $u = u^* U$, etc., we obtain:

$$\frac{U}{L}\left(\frac{\partial u_1{}^*}{\partial x_1{}^*}\right) + \frac{V_s}{\delta}\left(\frac{\partial u_2{}^*}{\partial x_2{}^*}\right) = 0 = \frac{\partial u_1{}^*}{\partial x_1{}^*} + \frac{V_s L}{\delta U}\left(\frac{\partial u_2{}^*}{\partial x_2{}^*}\right) \tag{8.6}$$

where the last set of terms is a consequence of dividing the first set of terms through by $\frac{U}{L}$. The coefficient of the first term become one, the coefficient multiplying the second term becomes $\frac{V_s L}{\delta U}$. At this point we apply an order of magnitude analysis of the terms. Both terms have to balance each other in the equation, being of opposite sign. We use the nomenclature $\mathcal{O}(1)$ to indicate that the value of a term is "order one". By proper scaling of the variables we assume that, $\frac{\partial u_1{}^*}{\partial x_1{}^*}$, is $\mathcal{O}(1)$. That is to say, by proper scaling this derivative using scales that are approximately the maximum value of the variable then the resultant term will not be a very large or a very small number, but rather "order one". We make the same assumption for the derivative $\frac{\partial u_2{}^*}{\partial x_2{}^*}$. Consequently since neither of these derivatives are zero, as we have noted previously for the boundary layer, then for this equation to be valid we must have

$$\frac{V_s L}{\delta U} = \mathcal{O}(1)$$

With this we can assign the value of the u_2 velocity scale to be:

$$V_s = U\frac{\delta}{L} \tag{8.7}$$

By doing so then each term is $\mathcal{O}(1)$. Keep in mind that we are not trying to find exact values but at this point trying to determine approximately how large or small the scaling values should be. If we now take Equation (8.7) and insert this into Equation (8.6) we end up with:

$$\left(\frac{\partial u^*}{\partial x^*}\right)+\left(\frac{\partial v^*}{\partial y^*}\right)=0 \tag{8.8}$$

for the nondimensional representation of the conservation of mass with the scaling of the variables given by the relationships above.

Using our new found scaling for u_2 we continue this same non-dimensional process for the other terms in the Navier-Stokes Equation (8.2). That is, replacing all of the variables with the nondimensional variables, and then dividing the resulting equation by the coefficient of the first term, $\frac{\rho U^2}{L}$ resulting in:

$$u_1{}^*\frac{\partial u_1{}^*}{\partial x_1{}^*}+u_2{}^*\frac{\partial u_1{}^*}{\partial x_2{}^*}=\frac{\mu}{\rho UL}\left(\frac{\partial^2 u_1{}^*}{\partial x_1{}^{*2}}+\frac{L^2}{\delta^2}\frac{\partial^2 u_1{}^*}{\partial x_2{}^{*2}}\right) \tag{8.9}$$

This nondimensional equation, that incorporates the scaling given above, leads to some profound conclusions. First note that the coefficient on the right hand side of the two terms in parentheses, which are the fluid friction terms, is the inverse of the Reynolds number that we define for boundary layer flows: $Re_L=\frac{\rho U_\infty L}{\mu}$. This Reynolds number is based on the freestream velocity and the total length of the surface. We have included a subscript L on the Reynolds number to inform us of the selected length scale. Next we have the coefficient $\frac{L^2}{\delta^2}$ of the last term in parentheses. Since we have assumed that the boundary layer is thin ($\delta \ll L$) then this coefficient will be large. Since each of the derivatives is assumed to be order one through proper scaling, then the entire second term in parentheses must be much larger than the first term, or:

$$\frac{\partial^2 u_1{}^*}{\partial x_1{}^{*2}} \ll \frac{L^2}{\delta^2}\frac{\partial^2 u_1{}^*}{\partial x_2{}^{*2}} \tag{8.10}$$

So the frictional forces in the boundary layer are dominated by the term containing $\frac{\partial^2 u_1{}^*}{\partial x_2{}^{*2}}$. This term is the net angular deformation caused by shearing stress. The first term is the linear deformation caused by the normal viscous stress. This result is consistent with the fact that the thin boundary layer will have very large derivatives of velocity in the x_2 direction when compared with the x_1 direction. So neglecting the normal viscous stress contribution the resulting nondimensional form of the boundary layer equation for steady flow over a flat surface is:

$$u_1{}^* \frac{\partial u_1{}^*}{\partial x_1{}^*} + u_2{}^* \frac{\partial u_1{}^*}{\partial x_2{}^*} = \frac{\mu}{\rho U L} \left(\frac{L^2}{\delta^2} \frac{\partial^2 u_1{}^*}{\partial x_2{}^{*2}} \right) \tag{8.11}$$

There is one more conclusion that can be arrived at from this scaling. Noting that the shearing contribution derivative, $\frac{\partial^2 u_1{}^*}{\partial x_2{}^{*2}}$, is $\mathcal{O}(1)$ as are each of the nondimensional acceleration terms on the left hand side, then in order for this equation to be balance $\left(\frac{\mu}{\rho U L} \frac{L^2}{\delta^2} \right)$ should also be $\mathcal{O}\,(1)$:

$$\frac{\mu}{\rho U L} \left(\frac{L^2}{\delta^2} \right) \sim \; \mathcal{O}(1)$$

or

$$Re_L \sim \frac{L^2}{\delta^2} \tag{8.12}$$

This last condition implies that for a thin boundary layer to exist the Reynolds number should be large. So for large Reynolds numbers in boundary layer flows with a surface length of L the boundary layer thickness, δ, is proportional to the square root of Re_L which we can write as:

$$\frac{\delta}{L} = \frac{C}{\sqrt{Re_{x_1}}} \tag{8.13}$$

where C is some unknown constant inserted to make the equation quantitatively correct. Consequently, for very small values of L the boundary layer conditions do not hold since Re_L is small.

The nature of the governing equation given by Eqn. (8.11) is that it is a parabolic partial differential equation. Since it only requires one boundary condition in x_1, which can be selected at $x_1 = 0$ (the leading edge) where the velocity is given as U, then the solution is independent of any downstream boundary condition. This means it can be solved at any arbitrary position x_1 along the surface. This also implies that the result (8.13) is valid by replacing L with location x_1. . Doing this we have a Reynolds number based on any position x_1:

$$Re_{x_1} = \frac{\rho U x_1}{\mu}$$

and Equation (8.13) can be expressed as:

$$\frac{\delta}{x_1} = \frac{C}{\sqrt{Re_{x_1}}} \tag{8.14}$$

Equation (8.14) predicts that the boundary layer grows proportional to the distance ${x_1}^{1/2}$ (recall that there is a factor x_1 contained in the Re_{x_1}); also this will not be valid for very small values of x_1.

Using Eqn. (8.12) the final form of the boundary layer equation for flow over a flat surface is:

$$u_1{}^* \frac{\partial u_1{}^*}{\partial x_1{}^*} + u_2{}^* \frac{\partial u_1{}^*}{\partial x_2{}^*} = \frac{\partial^2 u_1{}^*}{\partial x_2{}^{*2}} \tag{8.15}$$

From our discussion of the characteristics of the boundary layer we have the following boundary conditions:

(i) $x_2 = 0 : u_1 = 0, u_2 = 0$ (no-slip),

(ii) $x_2 = \delta : u_1$ = U

(iii) $x_1 = 0 : u_1$ = U

This equation seems to have eliminated all parameters (like viscosity, density and Re). However, recall that x_2 is non-dimensionalized using δ and also u_2 is non-dimensionalized using δ. In order to determine δ one needs to know the relationship between δ and Re. So even though we may be able to solve Eqn. (8.15) there is still work to do to interpret the results.

Laminar Boundary Layer Solution

The solution to the boundary layer equations for steady flow over a flat surface parallel with the oncoming flow, with the associated boundary conditions, is called the Blasius solution. This was accomplished around 1913 originally by Paul Blasius, a graduate student of Prandtl's. Noting that Eqn. (8.15) shows that the basic equation consists of two convective acceleration terms and one viscous term which can be written in terms of the original dimensional variables as:

$$\rho \left(u_1 \frac{\partial u_1}{\partial x_1} + u_2 \frac{\partial u_1}{\partial x_2} \right) = \mu \left(\frac{\partial^2 u_1}{\partial x_2} \right) \tag{8.16}$$

with the conservation of mass as Equation (8.3).

Following the general solution approach of Blasius we can introduce the streamfunction, and use it to replace the velocity components:

$$u = \frac{\partial \psi}{\partial x_2}; \quad v = -\frac{\partial \psi}{\partial x_1} \tag{8.17}$$

We have previously shown that this definition for two dimensional, incompressible flow satisfies conservation of mass, by inserting these expressions into Equation (8.3). Substituting these two expressions in terms of ψ for the two velocity components in Equation (8.16) results in:

$$\frac{\partial\psi}{\partial x_2}\left(\frac{\partial^2\psi}{\partial x_1\partial x_2}\right)-\frac{\partial\psi}{\partial x_1}\left(\frac{\partial^2\psi}{\partial x_2^2}\right)=\nu\left(\frac{\partial^3\psi}{\partial x_2^3}\right) \tag{8.18}$$

Here we have also divided through by density to obtain the kinematic viscosity, $\nu = \mu/\rho$, as the coefficient of the viscous term which is the only parameter in the equation (a constant for a given fluid). Although the resulting equation seems formidable the use of the streamfunction has reduced the two velocities into a single dependent variable ψ.

The streamfunction, with SI units of m^2/s, is nondimensionalized as:

$$f\left(\eta\right)=\frac{\psi}{\left(\nu x_1 U\right)^{\frac{1}{2}}} \tag{8.19}$$

a non-dimensional similarity variable, η, is defined to combine x_1 and x into a variable:

$$\eta=\frac{x_2}{\left(\frac{\nu x_1}{U}\right)^{1/2}}=x_2\left(\frac{U}{\nu x_1}\right)^{1/2} \tag{8.20}$$

The new variable f is assumed to be only a function of η. This will be verified by inserting these new variables into the original equation and see if the result is only η dependent. Each of the terms in Eqn. (8.18) are transformed into the (f,η) variables using the chain rule similar to what was done in chapter 7 to determine the governing equation for a suddenly accelerated flat surface. Similarly, the non-dimensional stream function of Eqn. (8.18) can be written in terms of u_1 and u_2 and inserted into Eqn. (8.16). The result is the following, using the prime designation to represent the derivative with respect to η

$$u_1=\frac{\partial\psi}{\partial x_2}\frac{\partial\psi}{\partial\eta}\frac{\partial\eta}{\partial x_2}=\frac{\partial\psi}{\partial\eta}\left(\frac{U}{\nu x_1}\right)=f'U \tag{8.21}$$

$$u_2=\frac{U}{2\sqrt{Re_x}}(\eta f'-f) \tag{8.22}$$

$$\frac{\partial u_1}{\partial x_1}=\frac{\eta}{2}\frac{U}{x_1}f'' \tag{8.23}$$

$$\frac{\partial u_1}{\partial x_2}=Uf''\left(\frac{U}{\nu x_1}\right)^{1/2} \tag{8.24}$$

$$\frac{\partial^2 u_1}{\partial {x_2}^2} = \frac{U^2 f'''}{\nu x_1} \tag{8.25}$$

Substituting all of this into our boundary layer equation, (8.16), with a little bit of manipulation the result becomes:

$$f''' + \frac{1}{2} f f'' = 0 \tag{8.26}$$

This now is a single variable ordinary differential equation, which shows that $f = f(\eta)$ resulting in a similarity equation. To obtain a solution the boundary conditions need to be specified in terms of η. Specifically there are three: $x_2 = 0 : u_1 = u_2 = 0$ (no slip condition) so

$$f(0) = f'(0) = 0$$

$$x_2 \geq \delta : u_1 = U \text{ so}$$

$$f'(\eta \to \infty) = 1.0 \tag{8.27}$$

The no slip condition for u_2 results in $f(0) = 0$ since $f'(0) = 0$ for the no slip condition of u_1 so by Eqn. (8.22) $f(0) = 0$. Also, we take the boundary condition at the edge of the boundary as $\delta \to \infty$ since U remains constant for $x_2 > \delta$. Physically this imposes an asymptotic limit of the solution for large δ, or beyond the edge of the boundary layer.

The solution to Equation (8.26) along with the boundary conditions of Equations (8.27) is rather straight forward using a Runge-Kutta technique. However, this was not the case when Blasius solved this equation numerical by hand back in the early 1900s at the University of Göttingen.

The results of the numerical solution of Eqn (8.26) are expressed as $f'(\eta) = u_1/U_\infty$ and are shown in Figure (8.3). Obviously u_1/U varies from zero at the surface ($\eta = 0$) and approaches 1.0 at $x_2 = \delta$. The value of δ can be determined from this plot, however one must select a value of $f'(\delta)$ close to 1.0, and typically 0.99 is chosen. At this value of $f'(\delta)$ the value of $\eta \simeq 5.0$. Using the definition of η given above and setting it equal to 5.0 when $x_2 = \delta$ results in:

$$5 = \frac{\delta}{\left(\frac{\nu x_1}{U}\right)^{1/2}}$$

Rearranging this yields an expression for the boundary layer versus x_1:

$$\frac{\delta}{x_1} = \frac{5}{{Re_{x_1}}^{1/2}} \tag{8.28}$$

This shows that $C = 5$ in Eqn. (8.13). Eqn. (8.28) allows for the evaluation of the boundary layer thickness, δ, at any x_1 location for a given value of U and viscosity ν. Using the solution in Fig. (8.3) also allows for the evaluation of the velocity components, u_1 and u_2 and any location x_1 and x_2 in the boundary layer.

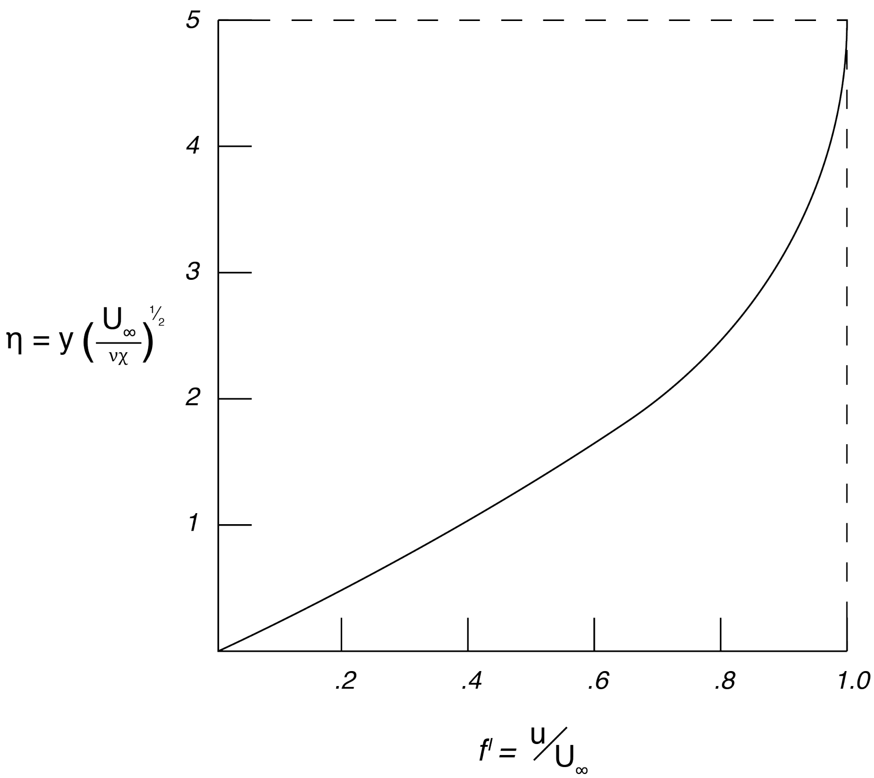

Fig 8.3 Blasius solution to steady laminar flow over a flat plate.

Other aspects of the flow can also be found from the solution. The total force on the surface caused by fluid flow friction can be found from the surface stress, $\tau_s = \mu \frac{\partial u_1}{\partial y}$, which requires evaluating the velocity derivative at the surface, x_2 = 0. The non-dimensional form is used to evaluate $\frac{\partial u_1}{\partial y}$ at $x_2 = 0$. Using Eqn. (8.24) we have:

$$\left(\frac{\partial u_1}{\partial x_2}\right)_{x_2=0} = f''(0) U^{3/2} \sqrt{\frac{\rho}{\mu x_1}} \tag{8.29}$$

where $f''(0)$ is the second derivative of *f* evaluated at $\eta = 0$. From the Blasius solution $f''(0) = 0.332$. After multiplying Equation (8.29) by the dynamic viscosity to obtain the surface stress and then dividing by $\frac{1}{2}\rho U^2$ which defines the surface skin friction coefficient, c_f, the result is:

$$c_f = \frac{\tau_s}{\frac{1}{2}\rho U^2} = \frac{0.664}{{Re_{x_1}}^{1/2}} \tag{8.30}$$

The above expression can be used to find the local surface stress at any x_1 location along the surface (recall $Re_{x_1} = \dfrac{\rho U_\infty x_1}{\mu}$). This then indicates that for a given freestream velocity of a given fluid the surface shear stress decreases as ${x_1}^{-1/2}$. The final step to determine the total drag force, F_D, on the surface is to integrate τ_s over the entire surface using the results of Equation (8.30). $F_d = \int_0^L \tau_s dx_1 S$ which is written as the drag coefficient, C_D:

$$C_D = \frac{F_D}{\frac{1}{2}\rho U^2 (LS)} = \frac{1.328}{{Re_L}^{1/2}} \tag{8.31}$$

where S is the span of the surface in the x_3 direction.

The drag coefficient provides a nondimensional convenient expression to determine the overall drag force on a surface. Knowing the length of plate, L, one calculates the Re_L and then uses (8.31) to find F_D.

Pressure Gradient Effects

The above discussion is concerned with forces caused by fluid friction for flow over a surface. The other major contribution to the total force acting on a surface when there is flow over the surface is that of pressure. When the pressure is uniform within the flow it has no contribution to the change of momentum of the flow (zero pressure gradient) along the flow. However, as we have seen for inviscid flow, a pressure distribution over a surface results in a force and this pressure distribution is significantly altered by the flow conditions. Consider flow over a cylinder or Rankine oval where the velocity variation results in a pressure variation at the surface of the oval. The force for inviscid flow can be obtained from the Bernoulli equation to evaluate the local pressure which is then integrated over the surface.

For viscous flows the pressure and surface frictional forces both need to be integrated over the surface. However, importantly, these two can not be treated as independent of each other. That is to say, the pressure distribution is influenced by the velocity distribution, or vice versa, as we see from the Navier-Stokes equation which contains a pressure gradient term. Consequently, one can expect that the velocity distribution within the boundary layer will be altered as the pressure gradient changes (in other words we no longer have Eqn. (8.3) which assumes $\dfrac{\partial P}{\partial x_1} = 0$). With an altered velocity profile the velocity gradient at the surface also changes indicating that the surface stress changes. The link between pressure gradient and surface stress can be very complex, influenced by the conditions that result in a specific pressure gradient.

This is made apparent by considering the Navier-Stokes equation evaluated at the surface, with no slip boundary conditions. In this case acceleration terms are all zero and there is a balance of pressure and viscous forces at the surface:

$$\frac{\partial P'}{\partial x_1} = \mu\left(\frac{\partial^2 u_1}{\partial {x_2}^2}\right)_{x_2=0} = \left(\frac{\partial \tau}{\partial x_2}\right)_{x_2=0} \tag{8.32}$$

For the boundary layer, assuming it is thin, the pressure gradient can be evaluated outside the boundary layer as discussed previously. Also, in this expression we have absorbed the body force term into the pressure term: $P' = P + \rho g h$ where *h* is the height above some datum. This form of the pressure plus body force accounts for the hydrostatic pressure variation that may occur along the direction x_1 caused by changes in elevation given by changes in *h*.

Eqn. (8.32) provides insight into the flow conditions very close to the surface for changing pressure gradients. For instance, if $\frac{\partial P'}{\partial x_1} < 0$ (a *"favorable pressure gradient"*) then the pressure decreases in the flow (or x_1) direction. This implies from Eqn (8.32) that the surface stress decreases moving away from the surface as one might expect since it ultimately reaches zero at the edge of the boundary layer, for inviscid flow conditions. For conditions of very large favorable pressure gradients ($\frac{\partial P'}{\partial x_1} \ll 0$) the decrease of stress with x_2 is greater and the boundary layer becomes thinner, and the wall shear stress becomes larger. The distribution of stress is shown in qualitatively Fig. 8.4.

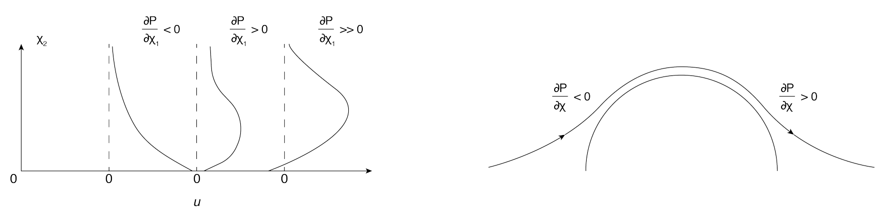

Fig 8.4 Stress distribution for favorable and adverse pressure gradients in boundary layer flows; flow over a cylinder illustrating favorable and adverse pressure gradients for flow over a cylinder.

If the pressure gradient has a positive sign, $\frac{\partial P'}{\partial x_1} > 0$, (an *"adverse pressure gradient"*) the stress increases with increasing x_2 away from the surface again as shown in Eqn. (8.32). This implies that at some point the stress reaches a maximum, and then decays to zero at the edge of the boundary layer. See Fig. 8.4. As the adverse pressure gradient increases one can suspect that the gradient of stress near the surface also becomes larger, forcing the stress to approach zero or even go negative as shown in Fig. 8.4. Under these conditions, of negative stress, the implications are that the sign reversal causes the flow in a region near the wall to actually go in the negative, or upstream, x_1 direction. This is the definition of "*flow separation*". Separated flow no longer adheres to boundary layer flow as part of the flow near the surface is moving upstream and part of the flow further from the surface is moving downstream. This generally results in swirling flow near the surface.

What can cause such a large adverse pressure gradient? One common situation is the existence of large surface curvature, such as flow over a cylinder of diameter D and length S into the page, shown in Fig. 8.5. In these cases the x_1 coordinate is taken as curving along the surface in the flow direction. On the upstream side of the cylinder the pressure gradient is negative as the flow accelerates with increasing velocity. The growth of δ is not as large as for the zero pressure gradient case, as noted above. As the flow continues over the top (or bottom) of the cylinder the pressure gradient becomes positive, increasing pressure in the flow direction. This is caused by the decrease of velocity for the flow beyond the top (bottom) of the cylinder. The inviscid flow over a cylinder has been studied previously (as a superposition of uniform flow and doublet). For this inviscid case the pressure can be found from the Bernoulli equation and the result can be expressed as the pressure coefficient as:

$$c_p = \frac{P - P_\infty}{\frac{1}{2}\rho U^2} = 1 - \frac{{v_s}^2}{U^2} = 1 - 4sin^2\theta \tag{8.33}$$

where P_∞ is the pressure for upstream (or downstream) of the cylinder and v_s is the surface velocity at any point around the cylinder (zero at the front and back stagnation points and maximum at the top and bottom). A plot of this inviscid pressure distribution around the cylinder is shown in Fig. 8.5. Notice that the pressure distribution is symmetric and the net force caused by pressure is zero. The maximum pressure is at the stagnation points, as expected, and equal to $P_\infty + \dfrac{1}{2}pU^2$ from Bernoulli equation.

With the addition of viscous effects, for flow over a cylinder, as described above, the adverse pressure gradient on the rear portion of the cylinder results in flow separation when the freestream flow is sufficiently large. The flow then forms a "wake" across the back of the cylinder consisting of swirling, turbulent flow. The result is an asymmetric flow pattern around the cylinder and an asymmetric pressure distribution. In the wake the pressure is not as high as in the inviscid case. We see in the pressure coefficient plot that for viscous flows the pressure recovery on the downstream side is not as large as the inviscid case and the net affect is a downstream drag force. Turbulent flows tend to have a greater pressure recovery and a lower nondimensional drag coefficient ($C_D = \dfrac{F_D}{\frac{1}{2}\rho U^2 DS}$) when compared with laminar flow.

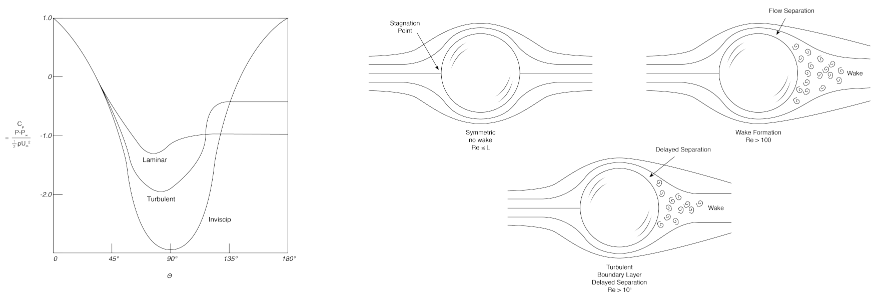

Fig 8.5 Pressure distribution for flow over a cylinder and illustration of wake formation for laminar and turbulent flow.

IX. INTEGRAL BOUNDARY LAYER RELATIONSHIPS

Historically, the development of the integral form of the boundary layer equations, as is presented here, has provided a powerful tool to evaluate surface viscous forces for more complicated flows with pressure gradients. In the Blasius solution presented in the last chapter, the velocity profile is determined directly from a modified form of the Navier-Stokes equation. From this solution, the local velocity derivative at the surface, and therefore the surface shear stress, can be found as a function of position along the surface. Using the definition of the surface stress the total force along the surface can then be found. The integral method in many ways takes the opposite approach. The basic governing equations are integrated across the flow using the wall shear stress as an unknown boundary condition, eventually to be solved for. The local pressure gradient, which may vary in the freestream velocity direction, is taken to be a parameter known at each position along the flow. This can be done since the assumption is that the pressure gradient in the freestream is identical to the pressure gradient in the boundary layer. This is part of the boundary layer assumptions and is valid for both laminar and turbulent flows. In arriving at the integral form of the boundary layer equations there are several scaling parameters introduced along the way that are often used to characterize the boundary layer flow and help interpret the flow conditions. These parameters can be used to help scale the flows and predict surface force distributions.

Scaling Parameters

Boundary layer thickness

The boundary layer thickness, as we have seen, is given by δ, and it represents the thickness of the boundary layer measured from the surface to the location where the velocity reaches the freestream value, U. However, since the velocity within the boundary layer asymptotically approaches U it is often difficult to obtain an accurate measure of δ. To circumvent this problem the boundary layer thickness can be taken to be when the velocity reaches, say, 1% of U. As discussed in the last chapter, in a favorable pressure gradient where the pressure decreases along the flow direction, the boundary layer will be thinner when compared with a zero pressure gradient. The additional pressure force in the flow direction increases the local velocity at any given position and the boundary layer reaches the freestream value at a lower value of the cross stream coordinate. This then reduces the boundary layer thickness. The opposite is true for an adverse pressure gradient. Consequently, the boundary layer thickness is directly influenced by the pressure gradient and as such there is a similar impact on the surface stress. A thinner boundary layer caused by a favorable pressure gradient, with the same freestream velocity, will have a larger surface velocity gradient and a higher local surface shear stress.

In general we note that the boundary layer thickness is a function of the downstream coordinate, x_1, and δ increases in the x_1 direction. An alternative way of expressing this is through the Reynolds number, since the Reynolds number depends on x_1 $\left(Re_{x_1} = \dfrac{\rho U x_1}{\mu}\right)$:

$$\delta = f(Re_{x1})$$

Displacement thickness, δ_1

The displacement thickness, δ_1, and momentum thickness, δ_2, are often used as a measure of the thickness of the boundary layer but are not actually the boundary layer thickness; these two are important parameters in the analysis of the frictional forces on the surface. The displacement thickness is, in general, a function of position, x_1, along the flow direction as is δ. Typically δ_1 increases with increasing x_1 and is less than δ. A sketch illustrating the definition of the displacement thickness is given in Fig. 9.1 where δ_1 is determined based on the mass flow rate within the boundary layer. The velocity distribution can be integrated across the boundary layer, normal to the surface, to determine the mass flow rate at any location, x_1 as

$$\dot{m} = \int_0^{\delta} \rho u_1 dx_2 \; S \tag{9.1}$$

where u_1 is the x_1 component of the velocity and S is the span, or the distance into the page. The distribution of u_1 follows the two boundary conditions, $u_1 = 0$ at the surface and $u_1 = U$ at the edge of the boundary layer, δ.

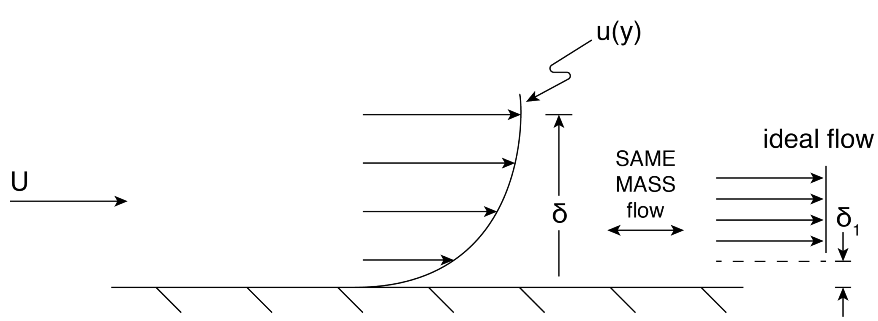

Fig 9.1 Illustration of the definition of the displacement thickness based on the total mass flow rate within the boundary layer; note that the mass flow rate changes along the flow in the x_1 direction consequently δ_1 is a function of x_1.

The surface generated friction by the surface on the flow causes the velocity to decrease at any given x_2 position along the surface. This decrease across the entire boundary layer results in a decreasing flow rate within the boundary layer with increasing x_1. Therefore the amount of mass flow lost in the boundary layer due to surface friction can be thought of as local a mass flow deficit. This deficit can be calculated by comparing the actual velocity distribution to the ideal velocity without friction, which would be U across the entire boundary layer. The local mass flow deficit at any x_2 location is then $d\dot{m}_{deficit} = \rho\,(U-u)\,dy\,S$ and the total mass flow deficit is obtained by integrating this across the flow as:

$$\int_0^\delta d\dot{m}_{deficit} = \dot{m}_{deficit} = \int_0^\delta \rho\,(U-u_1)\,dy\,S \tag{9.2}$$

The mass flow deficit can be equated to mass flow rate loss given as the product of density, U and (δ_1 S), where δ_1 is an unknown "thickness". So setting the integral term in Eqn. (9.2) to this product $(\rho U \delta_1 S)$ and solving for δ_1 results in:

$$\delta_1 = \int_0^\delta \left(1 - \frac{u_1}{U}\right) dy \tag{9.3}$$

which assumes that the density is constant. Eqn. (9.3) is the definition of the displacement thickness and can be interpreted as follows. If the total mass flow rate lost in the boundary layer due to friction is divided by ρUS the result is a length that would represent a distance normal to the surface through which all of the lost mass flow rate would pass if it traveled at velocity U(the velocity it would have if there were no friction.) Another way of looking at this distance is that it represents the vertical distance the surface would need to be moved upward (in the x_2 direction) to capture all of the lost mass flow rate if the velocity were uniformly at U, or frictionless. Either of these interpretations indicates that as δ_1 grows larger along the flow there is an increase in the total mass flow deficit. Since surface friction slows more and more fluid, creating a larger boundary layer thickness in the x direction, then δ_1 must increase in the downstream x_1 direction. At any given position along the surface the greater the local surface shear stress the greater the value of δ_1. Consequently, a favorable pressure gradient which increases the local shear stress compared with zero pressure gradient, results in a larger relative value of displacement thickness.

Momentum thickness, δ_2

The momentum thickness, δ_2, has somewhat of the same interpretation as δ_1, but it has to do with the momentum rate loss by the frictional forces, rather than the mass flow rate loss. In this case we develop a measure for the momentum rate loss, or momentum deficit, generated by friction. Noting that the momentum rate lost crossing a given vertical plan across the boundary layer is given by:

$$\int_0^\delta \rho u \left(U - u_1\right) dx_2 \; S \tag{9.4}$$

where $\rho u dx_2 \; S$ is the mass flow rate within an elemental area $dx_2 S$ and the expression $\left(U - u_1\right)$ is the momentum lost per mass flow rate. The product of these two terms integrated over the entire boundary layer δ is the momentum loss rate at any given x_1 position along the surface. Similar to what was done for the mass flow rate deficit, here we imagine that the momentum rate lost due to friction is equal to the mass flow rate through an area equal to $\left(\delta_2 S\right)$ with velocity U or

$$\rho U \delta_2 S U = \rho U^2 \delta_2 S = \int_0^\delta \rho u \left(U - u_1\right) dx_2 \; S$$

Dividing through by $\rho U^2 S$ yields the definition of the momentum thickness:

$$\delta_2 = \int_0^\delta \frac{u}{U}\left(1 - \frac{u_1}{U_\infty}\right) dx_2 \tag{9.5}$$

We can interpret this as the distance δ_2 the surface would need to be moved in the x_2 direction into the flow if the velocity is uniformly at U in order to reduce the momentum rate equivalent to the actual rate of momentum loss. We can also interpret this somewhat differently as follows.

A flat surface is shown in Fig. 9.2 indicating the surface shear stress, τ_s, acting on the fluid. A control volume with an elemental length along the surface, x_1, and extending upward to the edge of the boundary layer is shown in the figure. The sum of all of the forces acting on the fluid in the control volume consists of τ_s, since there is zero pressure gradient along the flow, and we assume there is no frictional forces at the top edge of the boundary layer, by definition of the extent of the boundary layer. The momentum equation for this control volume becomes the sum of the forces equal to the change of momentum rate leaving compared to that entering:

$$-\tau_s dx_1 S = \left(\rho U^2 \delta_2 S\right)_{x+dx_1} - \left(\rho U^2 \delta_2 S\right)_{dx_1} = \left(\rho U^2 d\delta_2 S\right) \tag{9.6}$$

where $d\delta_2$ is the change of the momentum thickness along dx_1, while noting that $\rho U^2 S$ is constant along x_1. The negative sign is included to indicate that the stress on the fluid is in the negative x_1 direction at the surface. If we rearranging this equation and change the stress to be that on the surface caused by the fluid flow (change the sign of τ_s) then:

$$\tau_s = \rho U^2 \frac{d\delta_2}{dx_1} \tag{9.7}$$

Note that this equation is valid for any particular velocity distribution that may exist in the boundary layer. Also, it indicates that the rate of change of the momentum thickness decreases along the flow direction since the surface stress decreases along the flow direction. If one can determine $\frac{d\delta_2}{dx_1}$ it is possible to find the wall surface stress, τ_s.

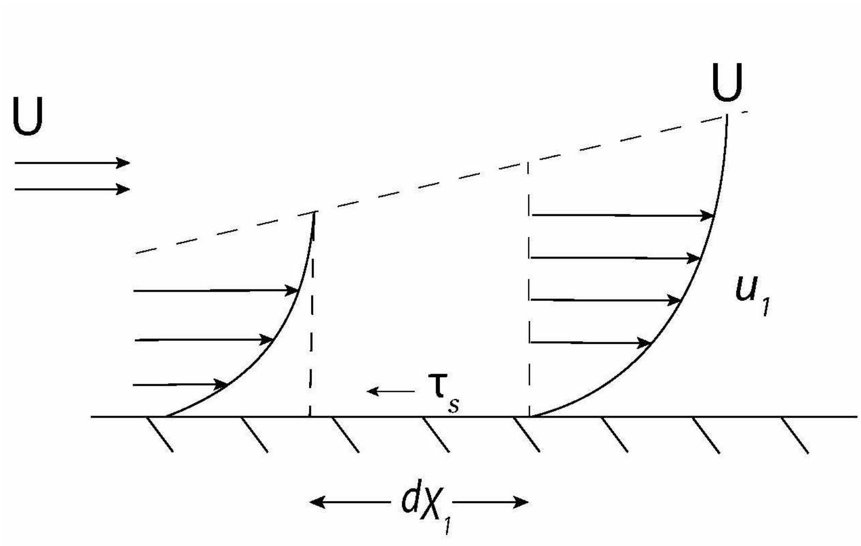

Fig 9.2

General Integral Boundary Layer Equations

The general integral boundary layer equation is obtained by starting with the Navier- Stokes equation simplified for boundary layer flow:

$$u_1 \frac{\partial u_1}{\partial x_1} + u_2 \frac{\partial u_1}{\partial x_2} = -\frac{1}{\rho} \frac{\partial P}{\partial x_1} + \nu \frac{\partial^2 u_1}{\partial x_2} \tag{9.8}$$

Note that $\nu = \frac{\mu}{\rho}$, and is the kinematic viscosity. Since the pressure gradient term can be determined from the freestream flow which is assumed to be inviscid the Euler equation can be used where we ignore gravitational effects such that:

$$-\frac{1}{\rho} \frac{\partial P}{\partial x_1} = U \frac{dU}{dx_1} \tag{9.9}$$

Note that body force terms could be included by replacing P with $P' = P + \rho gh$.

Equation (9.8) is integrated across the boundary layer, in the x_2 direction, for a given value of x_1. The boundary conditions for this are no-slip at x_2 = 0, and u = U at $x_2 = \delta$. Before we complete this operation we examine the second term on the left hand side in Eqn. (9.8). First we use continuity for a two dimensional flow:

$$\frac{\partial u_2}{\partial x_2} = -\frac{\partial u_1}{\partial x_1} \tag{9.10}$$

which integrates to:

$$u_2 = -\int_0^\delta \frac{\partial u_1}{\partial x_1} dx_2 \tag{9.11}$$

and this expression is used in the second term of (9.8). Next each term in Eqn. (9.8) is integrated from $y = 0$ to $y = \delta$. For instance the second term becomes:

$$\int_0^\delta u_2 \frac{\partial u_1}{\partial x_2} dx_2 = -\int_0^\delta \frac{\partial u_1}{\partial x_2} \left(\int_0^{x_2} \frac{\partial u_1}{\partial x_1} dx_2 \right) dx_2 \tag{9.12}$$

This term is now integrated by parts:

$$\int_1^2 b\ da = ab|_1{}^2 - \int_1^2 a\ db$$

where we set

$$db = \frac{\partial u_1}{\partial x_1} dx_2, da = \frac{\partial u_1}{\partial x_2} dx_2 = \partial u_1 \text{ and } a = u_1$$

The result for this term using the boundary conditions for u_1 is:

$$-U \int_0^\delta \frac{\partial u_1}{\partial x_1} dx_2 + \int_0^\delta u_1 \frac{\partial u_1}{\partial x_1} dx_2 \tag{9.13}$$

We insert (9.13) into (9.8) while integrating all other terms and obtain:

$$\int_0^\delta u_1 \frac{\partial u_1}{\partial x_1} dx_2 - U \int_0^\delta \frac{\partial u_1}{\partial x_1} dx_2 + \int_0^\delta u_1 \frac{\partial u_1}{\partial x_1} dx_2 = \int_0^\delta U \frac{dU}{dx_1} + \int_0^\delta \nu \frac{\partial^2 u_1}{\partial x_2} dx_2 \tag{9.14}$$

The last term is the viscous term and can be expressed in terms of the shear stress, $\tau = \mu \dfrac{\partial u_1}{\partial x_2}$ (the x_1 derivative of u_2 is taken to be small compared with the x_2 derivative of u_1, consistent with the boundary layer approximations.) So the last term is:

$$\int_0^\delta \nu \frac{\partial^2 u_1}{\partial x_2} dx_2 = \int_0^\delta \frac{1}{\rho} \frac{\partial \tau}{\partial x_2} dx_2 = \frac{1}{\rho} [\tau (x_2 = \delta) - \tau (x_2 = 0)] = -\frac{\tau_s}{\rho} \tag{9.15}$$

We combine the first and third terms of Eqn. (9.14) as:

$$\int_0^\delta 2u_1 \frac{\partial u_1}{\partial x_1} dx_2 = \int_0^\delta \frac{\partial\left(u_1 u_1\right)}{\partial x_1} dx_2 \tag{9.16}$$

Then we rewrite the second term of Eqn. (9.14) by bringing U inside the integral since it is not a function of x_2, but may be a function of x_1:

$$-U \int_0^\delta \frac{\partial u_1}{\partial x_1} dx_2 = \int_0^\delta \left(-\frac{\partial\left(uU\right)}{\partial x_1} + u\frac{\partial U}{\partial x_1}\right) dx_2 \tag{9.17}$$

Getting closer to the final result we combine all these expressions in (9.14) to obtain:

$$\int_0^\delta \left(\frac{\partial\left(u_1 u_1\right)}{\partial x_1} - \frac{\partial\left(u_1 U\right)}{\partial x_1} + u_1\frac{dU}{dx_1} - U\frac{dU}{dx_1}\right) dx_2 = \frac{\tau_s}{\rho} \tag{9.18}$$

This is rearrange as:

$$\int_0^\delta \frac{\partial\left(u_1\left(u_1 - U\right)\right)}{\partial x_1} dx_2 + \int_0^\delta \frac{dU}{dx_1}\left(u_1 - U\right) dx_2 = -\frac{\tau_s}{\rho} \tag{9.19}$$

Exchanging the order of integration and derivatives in the first term, changing sign of all the terms, yields:

$$\frac{\partial}{\partial x_1} \int_0^\delta u_1 (U - u_1) dx_2 + \frac{dU}{dx_1} \int_0^\delta \left(U - u_1\right) dx_2 = \frac{\tau_s}{\rho} \tag{9.20}$$

This now allows us to use the definitions of δ_1 and δ_2 to arrive at our final form as:

$$\frac{d}{dx_1}\left(U^2\delta_2\right) + \delta_1 U\frac{dU}{dx_1} = \frac{\tau_s}{\rho} \tag{9.21}$$

We end up with a differential equation in terms of the variables δ_1 and δ_2 both of which are functions of x_1. Recall that $U(x_1)$ is determined by the pressure gradient through use of Eqn. (9.9), Euler's equation. When U = constant, as in flow over a flat plate this equation can be simplified to:

$$\frac{d\delta_2}{dx_1} = \frac{\tau_s}{\rho U^2} \text{ or } 2\frac{d\delta_2}{dx_1} = \frac{\tau_s}{1/2\rho U^2} = c_f \tag{9.22}$$

where the right hand side is the skin friction coefficient.

The problem of determining the local surface stress distribution is now reduced to Eqn. (9.21) for flows over surfaces with a pressure gradient or (9.22) for a flat plate with no pressure gradient. Next, we will examine methods to arrive at solutions to this.

Solution Method

There are several methods available to arrive at a solution for Eqn. (9.21). We present a typical method that is based on the assumption of a velocity profile in nondimensional form across the flow at any given position, x_1. The key to this approach is based on the fact that the Blasius solution found a similarity solution and collapsed the velocity profile onto one curve when using proper scaling of the velocity and cross-stream coordinate, the latter also incorporated the stream-wise coordinate to help scale it properly. Here we will assume a non-dimensional velocity profile and use it to determine the integrals in the definitions of δ_2 and δ_1.

The proper scaling of the cross-stream coordinate is taken to be the boundary layer thickness, where δ is a function of x_1 then this scaling combines the cross-stream and stream-wise dependency. We define this new non-dimensional variable as:

$$\eta = \frac{x_2}{\delta} \tag{9.23}$$

being careful to note that this variable, η, is not the same as used in the Blasius definition. Next we assume that the nondimensional velocity, $f = \dfrac{u_1}{U}$, is some function of η or:

$$f = f(\eta) \tag{9.24}$$

One may say that it is necessary to precisely determine this function since the surface stress, τ_s, depends on the velocity derivative at the surface. This certainly is the case for the Blasius approach. However, examining Eqns. (9.21) and (9.22) it can be seen that the surface stress is a function of the integral of the velocity distribution as expressed through the variables δ_1 and δ_2. Based on this we conclude that to get a solution we must obtain good values for the integrals expressed in these equations, rather than the surface derivative of the velocity.

Taking this approach it is possible to assume a velocity distribution using the assumed nondimensional form in Eqn. (9.24) requiring it to satisfy the boundary conditions. One can use this distribution after transforming the integrals in (9.21) into the nondimensional form. We will use the example of flow over a flat plate, governing by Eqn. (9.22). This simplifies the details, but the same approach is used for flows with pressure gradients, but requires further input of a known pressure gradient.

First looking at Eqn. (9.22) written in terms of the skin friction coefficient we have:

$$c_f = 2\frac{d\delta_2}{dx_1} \tag{9.25}$$

We can not evaluate δ_2 since we do not know the value of δ. We illustrate the process by assuming a polynomial velocity distribution based on Eqn. (9.24) variables:

$$f = a + b\eta + c\eta^2 + d\eta^3 + \text{higher order terms} \tag{9.26}$$

There are four parameters in this polynomial, a, b, c and d that need to be determined based on boundary conditions on the velocity distribution. Notice that the higher the order of the polynomial the more conditions are needed to evaluate these coefficients. The boundary conditions written in terms of the variables, f, δ are:

$f(0) \;=\; 0$ (no slip boundary condition at the surface)

$f(1) \;=\; 1$ (velocity becomes the freestream value at δ)

$\dfrac{\partial f}{\partial \eta}(1) = 0$ (no shear at δ)

$\dfrac{\partial^2 f}{\partial \eta^2}(0) = 0$ (no net viscous force at $y = 0$)

The last condition is a consequence of all terms in the Navier-Stokes equation becoming zero at the surface if the pressure gradient is zero, and $u_1 = u_2 = 0$, and then transforming the viscous term into the non-dimensional variables. These four conditions can now be used to determine the four coefficients in Eqn. (9.26). The results are:

$$a = 0, \;\; b = 3/2, \;\; c = 0, \;\; d = -1/2$$

Inserting these into Eqn. (9.26) results in the velocity distribution:

$$f = \frac{3}{2}\eta - \frac{1}{2}\eta^3 \tag{9.27}$$

This result is unique to the selection of a third order polynomial for the velocity distribution. Next, we rewrite the relationship of c_f in terms of the nondimensional variables.

First we define the displacement and momentum thicknesses in terms of δ as:

$$\frac{\delta_1}{\delta} = \int_0^1 \left(1 - \frac{u_1}{U}\right) d\eta \tag{9.28}$$

$$\frac{\delta_2}{\delta} = \int_0^1 \frac{u_1}{U}\left(1 - \frac{u_1}{U}\right) d\eta \tag{9.29}$$

Here we have changed the integration from dx_2 to $d\eta$, where $dx_2 = \delta d\eta$ and need to change the limits of the integral accordingly. Notice that once we have an expression for $f = \frac{u_1}{U}$ from our polynomial, Eqn. (9.26), then both $\frac{\delta_1}{\delta}$ and $\frac{\delta_2}{\delta}$ are just constants. The important point now is that we can rewrite Eqn. (9.25) as:

$$c_f = 2\frac{d\delta_2}{dx_1} = 2\frac{d}{dx_1}\left(\left(\frac{\delta_2}{\delta}\right)\delta\right) = 2\left(\frac{\delta_2}{\delta}\right)\frac{d\delta}{dx_1} \tag{9.30}$$

So we have replaced having to know $\delta_2 = f(x_1)$ to needing to know $\delta = f(x_1)$. We find the latter relationship using our function $f(\eta)$ as:

$$\tau_s = \mu\frac{\partial u_1}{\partial x_2} = \mu\frac{\partial u_1}{\partial \eta}\frac{\partial \eta}{\partial x_2} = \frac{\mu U}{\delta}\frac{\partial f}{\partial \eta} = \frac{\mu U}{\delta}f'(0)$$

$$c_f = \frac{\tau_s}{\frac{1}{2}\rho U^2} = 2\frac{\delta_2}{\delta}\frac{d\delta}{dx_1} = \frac{\mu U}{\delta\frac{1}{2}\rho U^2}f'(0) \tag{9.31}$$

This last relationship is a differential equation for $\delta = f(x_1)$ since $\frac{\delta_2}{\delta}$ and $f'(0)$ are both constants known from Eqn. (9.26) using the boundary conditions to obtain Eqn. (9.27). Notice that these two constants are dependent on the order of the polynomial selected. Now Eqn. (9.31) can be integrated to obtain:

$$\frac{\delta}{x_1} = \frac{\left(2f'(0)\frac{\delta}{\delta_2}\right)^{1/2}}{{Re_{x_1}}^{1/2}} = \frac{C}{{Re_{x_1}}^{1/2}} \tag{9.32}$$

where $C = \left(2f'(0)\frac{\delta}{\delta_2}\right)^{1/2}$ and is a constant dependent on the order of the polynomial selected. Knowing $\delta = f(x_1)$ we can find $\frac{d\delta}{dx_1}$ and then c_f using Eqn. (9.31). The result is:

$$c_f = \frac{\delta_2}{\delta}\frac{C}{{Re_{x_1}}^{1/2}} \tag{9.33}$$

For our velocity profile, Eqn. (9.27) we have:

$$\frac{\delta_1}{\delta} = \frac{3}{8}, \frac{\delta_2}{\delta} = \frac{117}{840}, \text{ and } f'(0) = \frac{3}{2}$$

This results in $C = 4.64$ and:

$$c_f = \frac{0.6464}{(Re_x)^{1/2}} \tag{9.34}$$

The overall solution procedure now becomes pretty straight forward: (i) assume a functional form for $f(\delta)$, (ii) match required boundary conditions to find the coefficients in the equation, (iii) calculate the constant $\frac{\delta_2}{\delta}$, (iv) calculate the constant $f'(0)$, (v) finally calculate c_f, which determines the local value of the skin friction coefficient.

To determine the total friction drag force, F_D, on a surface of length L and area A_s = *LS* one needs to integrate the local surface stress along the distance L. The result is typically written in terms of the overall friction drag coefficient, C_f as:

$$C_f = \frac{F_D}{\frac{1}{2}\rho U^2 A_s} = \frac{1}{\frac{1}{2}\rho U^2 A_s}\int_0^L \tau_s dx_1 w = \frac{1}{L}\int_0^L c_f dx_1 = 2c_f(x_1 = L) \tag{9.35}$$

where the last designation, $2c_f(x_1 = L)$, means two times the value of the skin friction coefficient evaluated at $x_1 = L$.

The result assuming the third order polynomial for the non-dimensional velocity profile given above is:

$$C_f = \frac{1.2928}{{Re_L}^{1/2}} \tag{9.36}$$

The results when compared with experimental data for the appropriate Reynolds number conditions become very close to these predicted values. Consequently, this procedure is a fairly easy yet surprisingly accurate means to predict friction drag forces on flat surfaces. When pressure gradients come into play, such as surfaces with some degree of curvature it is more of a challenge to obtain a good velocity profile since for this case at the surface the net viscous forces are not zero but are balanced by the pressure gradient. The velocity profiles need to reflect this condition and there are a number of procedures available to address this. The interested reader is encouraged to see F.W. White's book, Viscous Fluid Flow for some examples.

X. INTRODUCTION TO TURBULENCE EFFECTS

The physical attributes of turbulent flow, in and of itself is a very difficult subject. That is to say, the flow characteristics of turbulence are difficult to measure, difficult to interpret and very difficult to incorporate into analyses. Never-the-less progress has been made, but much of it relies heavily on empirical results. Turbulence is typically described as a time varying phenomena of all dependent variables (except density for incompressible flows). In addition, spatial variations of the time dependency occurs as well. The results are that all of the velocity components and the pressure have spatio-temporal variations. Since the Navier-Stokes equations are nonlinear (through the convective acceleration terms) the statistical description of the flow relies on correlation functions among the various variables. There are a number of books written on the mathematical description of turbulence that can be challenging to incorporate into engineering applications. The nonlinear effects and some of the statistical measures of turbulence will become obvious once we look at the governing equations. For our purposes we will look at some of the physical consequences of turbulent flows and then illustrate how turbulent effects can be incorporated into an analysis of the viscous forces in boundary layer flows.

A few examples of turbulent flows are shown in Fig. 10.1. There are a wide range of fluctuations both in space and time. By scales we mean the magnitudes of local variations in time and space attributed to turbulent fluctuations about some local mean value. These are referred to as a broad spectrum of scales occurring within the flow. The flow geometry can have a large impact on the larger scales within the flow, since they interact often with the boundaries. However, the smaller scales tend to be mostly independent of the flow geometry indicating that there may be some underlying theoretical basis for their flow dynamics.

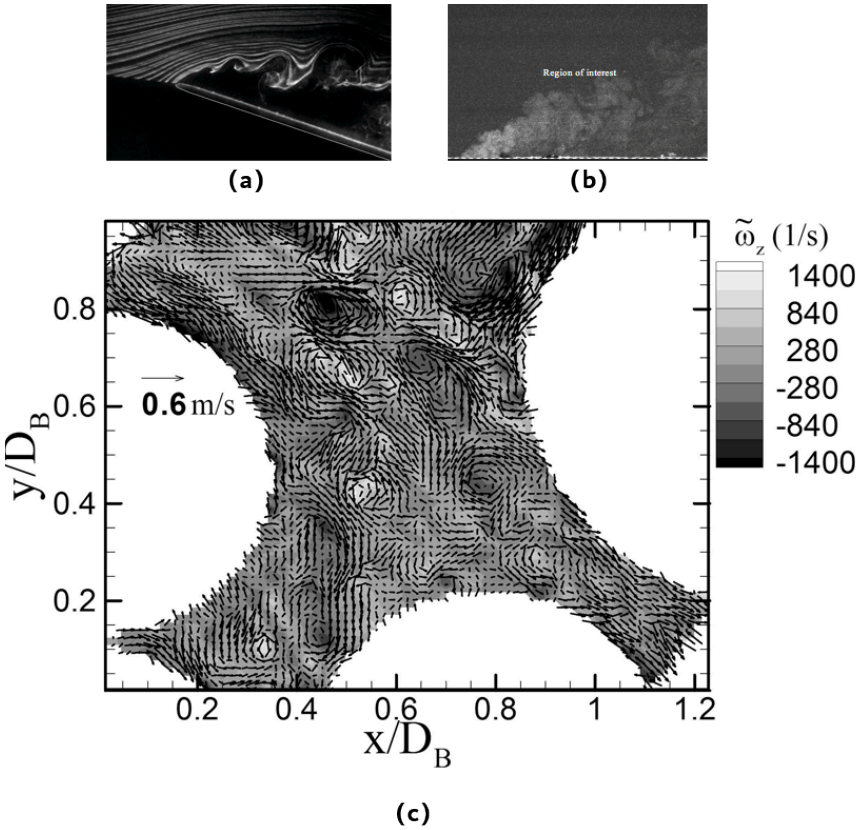

Fig 10.1 Illustrations of turbulence flow visualization; **(a)** smoke visualization of flow over an inclined wing indicating flow separation from the leading edge which transitions to turbulence; **(b)** smoke visualization from a turbulent jet injecting flow into a cross flow in a wind tunnel indicating large and small scale fluctuations; **(c)** particle image velocimetry (PIV) of flow in a porous media (through a random packing of spherical beads) showing instantaneous velocity vector distribution indicative of small scale swirling motion.

Shown in Fig. 10.2 is a typical time history signal of a measured velocity component say from a hot wire anemometer at a given location within the flow. Although this signal may seem random in nature, it has been learned that there is a lot of structure to these kinds of signals. One thing to notice is that there are time events happening over many different time scales. There are small scale (or short) events with relative small fluctuating values coupled with longer time varying, higher amplitude fluctuations. The short time events seem to be superimposed over the longer events. To help illustrate this variation of time scales Fig. 10.2 also illustrates the “energy spectrum” of the time series signal. Here the mean square value of the fluctuations are decomposed by using a Fourier transformation of the signal. The mean square fluctuations have units of velocity squared that can be interpreted as the kinetic energy per mass of fluid. This plot identifies the frequency dependency of the energy associated with the signal. We see that the larger amplitude fluctuations occur at the longer time scales (lower frequency) and the smaller amplitude fluctuations occur at the shorter time scales (higher frequency). Turbulent flows are characterized by a broad spectrum within the signal typically with large amplitude (or energy) fluctuations having low frequency and low amplitude high frequency components. Looking at Fig. 10.2 we see that the longer time scales have several orders of magnitude greater energy than the smallest scales. This distribution has implications concerning the mixing characteristics of turbulent flows such as in the ability to promote high reaction rates in combustion and other chemical reactions. In contrast the energy spectrum of a flow that has a single oscillating frequency would have an energy spectrum that would appear as a spike at the frequency of oscillation and would not be referred to as turbulent.

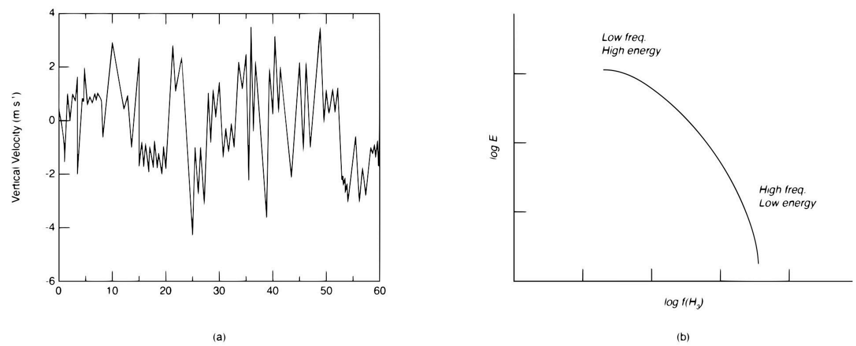

Fig 10.2 (a) Typical velocity signal of a single component of velocity in turbulent flow measured as a given location, notice the large and small scale fluctuations that are superimposed on the signal; **(b)** energy spectrum on a log-log scale of the mean square velocity fluctuations verses frequency of fluctuations, notice the large range of energy and frequency that occurs.

The integration of the energy spectrum over all frequencies yields the total energy of the fluctuations in the signal. This is equivalent to the time average of the square of the fluctuations (the mean square value) $\overline{u'^2}$, where the fluctuating velocity is $u' = (u - \overline{u})$ with $\overline{u}$ being the time average value of the velocity and u is the instantaneous value of the velocity. This can be used to define the "turbulent intensity" as:

$$\frac{\overline{\left(u'^2\right)}^{1/2}}{\overline{u}} = \text{"turbulent intensity"}$$

Notice that $\overline{u'^2}$ is obtained for a single velocity component, say u_1, so this represents the turbulent intensity of one component. If we calculate the mean square value for each component the total energy, known as the turbulent kinetic energy ("tke") is:

$$tke = \frac{1}{2}\left(\left(\overline{u'_1{}^2}\right) + \left(\overline{u'_2{}^2}\right) + \left(\overline{u'_3{}^2}\right)\right) \tag{10.1}$$

The greater the tke typically the more intense is the turbulence. This measure of turbulence can be measured at each location within the flow to determine the spatial distribution of turbulence in a time averaged sense.

Reynolds Averaging

The concept of time averaging of the terms in the Navier-Stokes equation after the velocity is decomposed into a mean and time varying component is known as Reynolds averaging. The instantaneous velocity can be expressed as the sum of the fluctuating part and the mean value at any point in the flow as shown above an rewritten here slightly differently:

$$u = (u' + \overline{u}) \tag{10.2}$$

where the primed quantity is the fluctuating value, which is time dependent, and $\overline{u}$ is the time average value. It should be noted that the time average of the fluctuating part is by definition zero. Each of the time dependent terms in the conservation of mass (or continuity equation) and Navier-Stokes equations can be replaced with the right hand side of Eqn. (10.2). Then each term is time averaged. For instance in the convective acceleration term:

$$\overline{u_j \frac{\partial u_i}{\partial x_j}} = \overline{(u_j{}' + \overline{u_j}) \frac{\partial \left(u_i{}' + \overline{u_i}\right)}{\partial x_j}} = \overline{u_j{}' \frac{\partial u_i{}'}{\partial x_j}} + \overline{u_j} \frac{\partial \overline{u_i}}{\partial x_j} \tag{10.3}$$

Where the two terms containing products of the mean and fluctuating parts, when time averaged, are zero since the time average of the fluctuations in zero.

The last term in Eqn. (10.3) is merely the convective acceleration using the time average velocities. Notice that the time averaging and the spatial derivatives can be interchanged. The first term on the very right hand side is the time average of the convective acceleration of the fluctuating velocities. This term is not necessarily zero for a term consisting of the product of two or more time varying signals. This is because the average of the products of time varying signals is not equal to the product of the averages of those signals. Let's examine this term a bit closer for incompressible flow we can write.

$$\overline{u_j{}' \frac{\partial u_i{}'}{\partial x_j}} = \frac{\partial \overline{(u_i{}' u_j{}')}}{\partial x_j} \tag{10.4}$$

Where, for incompressible flow, we are able to bring the velocity u_j inside the derivative with respect to x_j from the continuity condition for incompressible flows. This term can be interpreted as the spatial derivative of the correlation function $\left(\overline{u_i{}' u_j{}'}\right)$ that is the time averaged product of the various velocity components. This is a second order tensor with six independent components since it is a symmetric tensor.

This quantity, $\left(\overline{u_i{}' u_j{}'}\right)$ represents the contribution of turbulence to the mean momentum of the flow. That is to say, we have found a term that can change or adjust the mean momentum distribution in the flow caused by averaging the Reynolds decomposition of convective acceleration terms. We will see how this term affects the wall shear stress acting on the fluid for turbulent flow conditions.

Based on our earlier introduction of the turbulent kinetic energy, tke, one might expect that increased levels of tke would be associated with an increased magnitude of $\left(\overline{u_i{}' u_j{}'}\right)$ and increase the effect on the mean momentum distribution. How this occurs and under what conditions it occurs is not a simply thing to determine. This is because the relationship of the energy content of the fluid fluctuations with the momentum transport properties of the turbulence is a set of complicated interactions. Never the less it is possible to observe trends of these interactions and to formulate models of how they work.

We further manipulate the time averaged Navier-Stokes equations by bringing the new fluctuating term $\left(\overline{u_i{}' u_j{}'}\right)$ over to the right hand side of the equation and group it with the viscous stress term:

$$\rho \overline{u_j} \frac{\partial \overline{u_i}}{\partial x_j} = -\frac{\partial \overline{P}}{\partial x_j} + \rho g_i + \left(\frac{\partial}{\partial x_j} \left(\mu \frac{\partial \overline{u_i}}{\partial x_j} - \rho \left(\overline{u_i{}' u_j{}'} \right) \right) \right) \tag{10.5}$$

Here we can see that the viscous term is combined with the momentum altering fluctuating term while all other terms are similar to the laminar flow equation except here we use the time average value of the variables. The last term has two contributions, the mean viscous stress term $\mu \frac{\partial \overline{u_i}}{\partial x_j}$, and the turbulence term. If we interprete the turbulence term as one that modifies the momentum distribution in the flow we can identify it as a "stress" and call it the "turbulent stress", τ_t and write it as:

$$\tau_t = -\rho \left(\overline{u_i{}' u_j{}'} \right) \tag{10.6}$$

In honor of Reynolds, who developed the Reynolds decomposition leading to this results this is often labeled the "Reynolds stress". We can write the total stress within the flow as:

$$\tau_{total} = \tau_{viscous} + \tau_{turbulent} = \mu \frac{\partial \overline{u_i}}{\partial x_j} - \rho \left(\overline{u_i{}' u_j{}'} \right) \tag{10.7}$$

In a number of situations the viscous stress is actually a lot smaller than the turbulent stress and can be ignored except maybe in certain region of the flow, say near a surface or object where the fluctuating quantities are dampened.

Turbulent Boundary Layer

The discussion that follows assumes that the flow is turbulent over the entire surface. The conditions for this are discussed later after this section. Similarly to what was done in laminar flow turbulent boundary layer flows can be analyzed using the same assumptions used to simplify the governing equations. Basically we assume the following for a two dimensional boundary layer flow:

- thin boundary layer, $\delta \ll$ L (or x)
- stream-wise velocity greater than the cross-stream velocity, $u_1 \gg u_2$
- cross-stream derivatives greater than stream-wise derivatives, $\dfrac{\partial}{\partial x_1} \ll \dfrac{\partial}{\partial x_2}$
- large Re_{x_1}

The resulting time averaged governing momentum equation becomes for constant property flows and ignoring the body force term:

$$\rho\overline{u_1}\frac{\partial\overline{u_1}}{\partial x_1} \quad \rho\overline{u_2}\frac{\partial\overline{u_1}}{\partial x_2} = -\frac{\partial\overline{P}}{\partial x_1} + \left(\frac{\partial}{\partial x_2}\left(\mu\frac{\partial\overline{u_1}}{\partial x_2} - \rho\left(\overline{u_1{}'u_2{}'}\right)\right)\right) \tag{10.8}$$

Here we have retained the pressure gradient term and only the mean pressure value remains after time averaging the mean plus fluctuating parts.

Notice that in the Reynolds stress term the only contribution is from what is called the "cross correlation", $\rho\overline{u_1{}'u_2{}'}$. This is a consequence of $\dfrac{\partial}{\partial x_1} \ll \dfrac{\partial}{\partial x_2}$ even though $\overline{u_1' u_1'}$ may be the same order of magnitude as $\overline{u_1' u_2'}$.

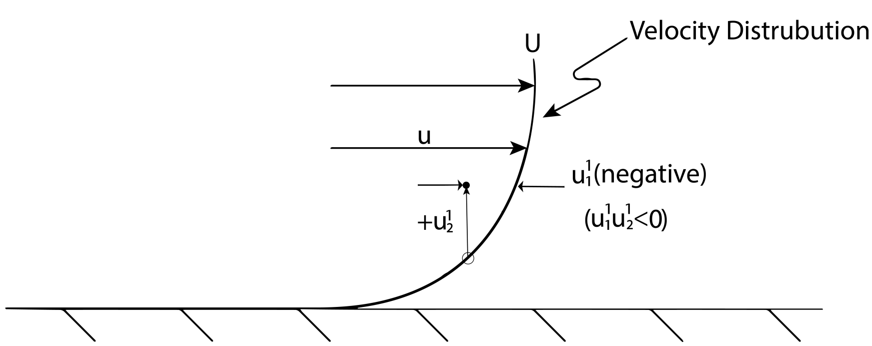

Fig 10.3 Representation of a positive fluctuating velocity in the x_2 direction resulting in a negative value of $u_1 u_2$.

The effect on the mean momentum distribution, caused by turbulence, then is brought about by the cross correlation contained in the Reynolds stress. Referring to Fig. 10.3 we attempt to provide some rationale for how this correlation may impact the momentum distribution and consequently the wall shear stress. At an instant in time imagine a positive, upward value of u_2. This moves fluid with a lower value of u_1 into a region of higher u_1 on average. Therefore the instantaneous value of ${u_1}'{u_2}'$ will be a negative number. Similarly if there is a negative value of u_2 it will move high u_1 velocity fluid into a slower moving region again causing ${u_1}'{u_2}'$ to be a negative number. Assuming this to be the case, one may assume that on average the value of $\overline{{u_1}'{u_2}'}$ is a negative number which means the added turbulent stress is positive, see Eqn. (10.6). This added stress slows down higher speed fluid and speeds up lower speed fluid. The result is a much flatter velocity or momentum distribution across the flow. However, the no-slip condition still holds true. This implies that on average the flatter velocity profile will have higher velocity gradients near the surface, such that the overall frictional force is larger. The net result is that a turbulent boundary layer is expected to have larger surface viscous stresses.

Scaling for Turbulent Boundary Layer Flows

We will define the displacement thickness, δ_1, and the momentum thickness, δ_2, identically as before for laminar flow except we use the time average values of velocity. However, we need to determine an appropriate method to scale the velocity to arrive at an accurate velocity distribution. As for laminar flow we can define the nondimensional cross-stream coordinate as: $\eta = \dfrac{x_2}{\delta}$. It turns out that the freestream velocity that was used to scale the stream-wise velocity in laminar flow may not be the best scale for the velocity within the boundary layer. The fairly flat velocity distribution of $\overline{u_1}$ in turbulent flow is heavily influenced by the velocity gradient near the wall that determines the wall shear stress. Consequently, a new velocity scale can be introduced that is proportional to the wall stress, called the "friction velocity":

$$v_f = \sqrt{\frac{\tau_s}{\rho}} \tag{10.9}$$

Notice that it is not a specific velocity within the flow but has units of velocity and is proportional to the velocity gradient at the surface through the value of the wall shear stress, τ_s. Since it is reasonable to note that the surface stress depends on the freestream velocity, one can also anticipate that $v_f = f(U)$.

From this we form the nondimensional velocity components:

$$u_1^{+} = \frac{\overline{u_1}}{v_f} \tag{10.10a}$$

$$u_2{}^+ = \frac{\overline{u_2}}{v_f} \tag{10.10b}$$

As we will see in the next section, this scaling of velocity can be used to arrive at an accurate near wall velocity distribution in non-dimensional variables. However, if we choose to try to determine the wall shear stress using an integral analysis similar to what was done in laminar flow, then we can use the following. First we assume a functional form:

$$\frac{\overline{u_1}}{U} = f(\eta) \tag{10.11}$$

In contrast to the polynomial distribution we used in laminar flow. We assume a power law instead of the polynomial (since it has been shown to match experimental data well) as:

$$\frac{\overline{u_1}}{U} = C\eta^{1/n} \tag{10.12}$$

where n is a positive integer and C is a constant. However, if we note that $\frac{\overline{u_1}}{U} = 1$ at η =1 then C = 1. Using this expression in the definitions for δ_1 and δ_2 we get:

$$\frac{\delta_1}{\delta} = \frac{1}{n+1} \tag{10.13}$$

$$\frac{\delta_2}{\delta} = \frac{n}{(n+1)(n+2)} \tag{10.14}$$

Experimental data shows that n is a weak function of Reynolds number, such that as Reynolds number increases the velocity profile becomes flatter and n increases. For moderately large Reynolds numbers n $\sim$ 7 matches data very well.

To go any further with this we need a relationship between τ_s and δ, similar to what was done with laminar flow, based on the nondimensional velocity distribution. For this we use an alternative scaling with a power law assumption given by:

$$u_1{}^+ = f_2(\frac{x_2 v_f}{\nu}) = C_2\left(\frac{x_2 v_f}{\nu}\right)^{1/n} \tag{10.15}$$

where C_2 is a constant and $\frac{\nu}{v_f}$ is a new length scale. At $x_2 = \delta$, we know that $\frac{\overline{u_1}}{U} = 1$ so we can write:

$$\frac{U}{v_f} = C_2\left(\frac{\delta v_f}{\nu}\right)^{1/n} \tag{10.16}$$

This provides the relationship between τ_s and δ, since τ_s is contained in v_f, see Eqn. (10.9). After inserting the definition of v_f and a little algebra we obtain:

$$\frac{\tau_s}{\rho U^2} = C_2^{-\frac{2n}{n+1}} Re_\delta^{-\frac{2}{n+1}} \tag{10.17}$$

where $Re_\delta = \dfrac{U\delta}{\nu}$ which represents a Reynolds number based on the boundary layer thickness.

Now we use the momentum integral equation that was derived for laminar flow, which is also valid for turbulent flow that yields for a flat plate:

$$c_f = 2\frac{\delta_2}{\delta}\frac{d\delta}{dx_1} = \frac{\tau_s}{\frac{1}{2}\rho U^2} \tag{10.18}$$

Noting that $\dfrac{\delta_2}{\delta}$ is a constant for a given value of n, and eliminating τ_s between Eqn. (10.17) and (10.18) and solving for δ we obtain:

$$\frac{\delta}{x_1} = C_T Re_{x_1}^{-\frac{2}{(n+3)}} \tag{10.19}$$

where

$$C_T = \left[\frac{\left(\frac{n+3}{n+1}\right) C_2^{\frac{-2n}{n+1}}}{\delta_2/\delta}\right]^{\frac{n+1}{n+3}}$$

that is fully determined by the constant C_2 and the value of n. Based on experimental data, much of it analyzed by Blasius for turbulent flow results in:

$$C_2 = 8.74 \tag{10.20}$$

Now we have Eqn. (10.19) fully determined so that we can find the derivative $\dfrac{d\delta}{dx_1}$ and inserts this into the expression for the skin friction, Eqn. (10.18). For the case of $n = 7$ we have:

$$\begin{aligned} C_T &= 0.37 \\ \frac{\delta_2}{x_1} &= 0.036\ Re_{x_1}^{-1/5} \\ c_f &= 0.0577\ Re_{x_1}^{-1/5} \end{aligned} \tag{10.21}$$

The determination of the total viscous drag force acting on the surface of length L and width S is obtained exactly as was done for laminar flow, by integration of the surface shear stress over the area. The results for the case of $n = 7$

$$C_f = \ 0.072\ Re_L{}^{-1/5} \tag{10.22}$$

$$F_D = C_f \frac{1}{2} \rho U^2 LS \tag{10.23}$$

Initial Laminar Starting Length

Turbulent flow over a surface in general will NOT exist from the beginning of the surface, x_1 = 0. Experiments haves shown that turbulent flow on a smooth surface occurs when the Reynolds number, Re_{x_1}, is greater than 5×10⁵. Since the Reynolds number is identically zero at the leading edge when x_1 = 0, there will be a region near the leading edge where laminar flow occurs, and then further along the surface the flow becomes turbulent if Re_{x_1} is large enough. Turbulent flow can occur from, or very close to, the leading edge if the flow is tripped. This occurs when there may be slight roughness near the leading edge and the freestream velocity is sufficiently large that turbulence occurs. Under these conditions the Eqns. (10.22) and (10.23) are valid over the entire length of the flow. For the conditions when the flow is not tripped the laminar starting region needs to be considered. A sketch of the boundary layer thickness as influenced by the initial laminar starting length and the transition to turbulence is shown in Fig. 10.4.

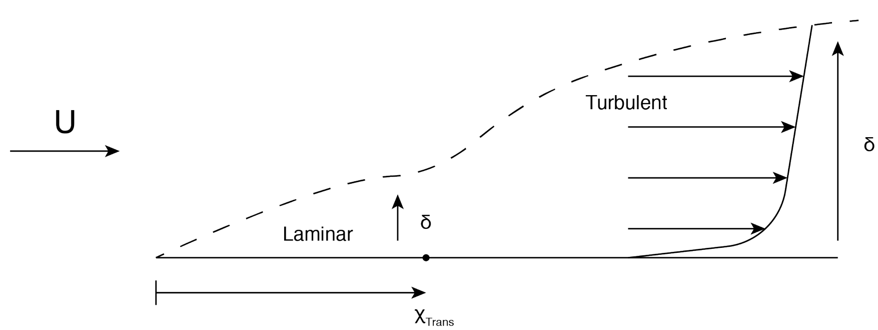

Fig 10.4 Illustration of the initial laminar starting length and how it influences the boundary layer thickness, transition occurs based on the critical Reynolds number, typically $Re_{crit} = 5x10^5 = Ux_{crit}/v$.

The solution to this situation of laminar flow up to the transition location along the surface and turbulent flow beyond this is obtained by dividing up the integration of the surface shear stress into laminar and turbulent regions. The location dividing the two regions is where $x = x_{transition}$ which is found using the critical Reynolds number.

$$x_{transition} = \frac{\left(5x10^5\right)\nu}{U} \tag{10.24}$$

Once the transition location is found then the integration over the entire surface becomes:

$$F_D = \int_o^{x_{transition}} \tau_s dx_1\ S\ + \int_{x_{transition}}^{L} \tau_s dx_1 S \tag{10.25}$$

Each term is now divided by $\frac{1}{2}\rho U_\infty{}^2(LS)$ to convert this equation into a nondimensional equation for C_D. The integrand for each term will be the skin friction coefficient, c_f and dx_1 becomes $d(x/L)$. There is a problem here though, the expression for c_f for the turbulent part (the second integral) can not be solved directly because the skin friction expression found previously assumes the flow begins turbulent at the leading edge. The solution to this problem is to recast the above integral by adding and subtracting the contribution to the total force from $x = 0$ to $x = x_{transition}$ based on turbulent flow. When this is added to the second term in Equation (10.25) the result is an expression for the force assuming turbulent flow from $x = 0$. The subtraction of this term in the first integral results in the difference between the laminar and turbulent generated force up until $x_{transition}$. Rearranging the terms results in

$$C_D = \int_0^L c_{f,\ turbulent}\, d\left(\frac{x}{L}\right) - \int_o^{x_{transition}} \left(c_{f,\ turbulent} - c_{f,\ laminar}\right) d\left(\frac{x}{L}\right) \tag{10.26}$$

By using the transitional location given in Eqn. (10.24) the second integral in Eqn. (10.26) can be found directly using the expressions for c_f. Writing this using Re_L (the Reynolds number evaluated at the end of the surface) results in:

$$C_D = \frac{0.072}{{Re_L}^{1/5}} - \frac{1700}{Re_L} \tag{10.27}$$

It should be noted that the above expression assumes $n = 7$. Also, if transition occurs at a slightly different Reynolds number the coefficient in the numerator of the second term in this equation will vary. The numerator of the second term may differ slightly based on the selected critical Reynolds number or power law exponent used.

Universal Velocity Profile

We now introduce the concept of the logarithm velocity profile in the near wall region of a turbulent boundary layer. This concept has proven to match experimental data very well and it is based on the premise that very close to the wall there is a constant shear layer. It also introduces the concept of a turbulent effective viscosity. If we take the stress term in the Navier-Stokes equation, Eqn. (10.7) for a boundary layer as:

$$\tau_{total} = \mu\frac{\partial \overline{u_1}}{\partial x_2} - \rho\left(\overline{u_1{}'u_2{}'}\right) \tag{10.28}$$

We assume that this stress is a constant which can be written in terms of the friction velocity, v_f. Then we model this term based on an effective viscosity, ν_t, that accounts for both the viscous and turbulent contributions which results in the total stress in terms of the friction velocity as:

$$\frac{\tau_{total}}{\rho} = v_f{}^2 = \nu_t\frac{\partial \overline{u_1}}{\partial x_2} \tag{10.29}$$

The effective viscosity (written here as a kinematic viscosity) has units of velocity times length. Taking the friction velocity as the appropriate velocity scale and x_2 as the appropriate length scale (since the viscous effects can only extend away from the wall some amount x_2) then we model the effective viscosity as:

$$\nu_t = \kappa v_f x_2 \tag{10.30}$$

where κ is an unknown constant. Inserting Eqn. (10.30) into (10.29) we have:

$$v_f{}^2 = \kappa v_f x_2\frac{\partial \overline{u_1}}{\partial x_2} \tag{10.31x}$$

This is now integrated in the x_2 direction for a constant value of v_f to obtain a velocity profile as:

$$\frac{\overline{u_1}}{v_f} = \frac{1}{\kappa}ln\ x_2 + c \tag{10.32}$$

This can easily be transformed into the following:

$$\frac{\overline{u_1}}{v_f} = \frac{1}{\kappa}ln\ \frac{x_2 v_f}{\nu} + B \tag{10.33}$$

where κ and B are constants determined from experimental results and shown to be $\kappa = 0.41$ and B = 5. Actually there are also theoretical arguments that can be made to show that $\kappa = 0.41$. This constant stress layer result is only valid fairly close to the surface, but has been shown over a wide range of conditions (different fluids, different Reynolds numbers, etc.) to be very accurate. The non-dimensional variable, $\dfrac{x_2 v_f}{\nu}$, is often given the symbol $x_2{}^+\ or\ y^+$, and $\dfrac{\overline{u_1}}{v_f} = u^+$, resulting in a non-dimensional velocity profile valid close to the wall that is expressed in terms of the wall shear stress contained in the variable u^+ and x_2^+.

This relationship for boundary layer flow of u^+ versus y^+ is shown in the figure below. Note that the region in which there is a log profile extends from approximately $x_2^+ = 30$ until the outer flow region is reached. The outer flow region is shown as a dashed line and begins further and further away from the wall (greater values of x_2^+) with increasing Reynolds numbers. Close to the wall ($x_2^+ < 30$) the turbulence is greatly suppressed by the wall and the log-profile is no longer valid. For $x_2^+ = 0 - 5$ the flow is dominated by viscous forces and it can be shown that $u^+ = y^+$ (a linear velocity profile). Pressure gradients along the wall are known to effect the outer region primarily.

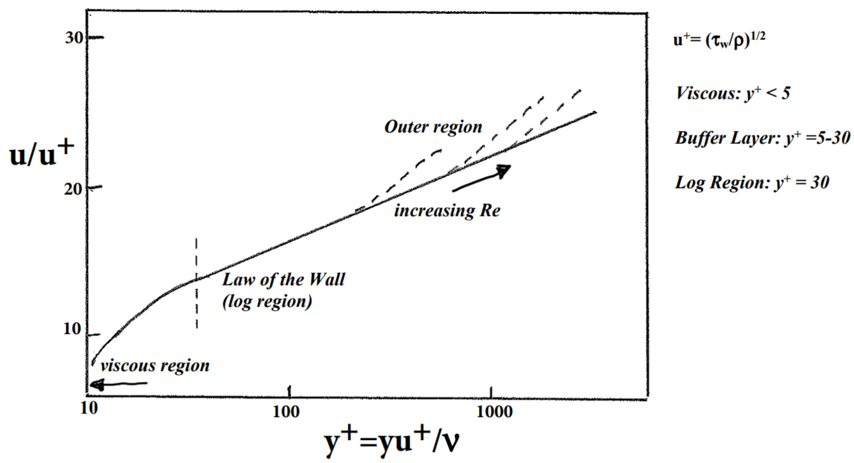

Fig 10.5

XI. BRIEF INTRODUCTION TO CFD BASICS

Why CFD

CFD (**c**omputational **f**luid **d**ynamics) attempts to solve the basic (differential) conservation equations. These include the conservation of mass equation:

$$\frac{\partial \rho}{\partial t} + \nabla \cdot (\rho V) = 0$$

and the conservation of momentum equation:

$$\rho \frac{\partial V}{\partial t} + \rho (V \cdot \nabla) V = -\nabla p + \rho g + \nabla \cdot \tau_{ij}$$

This set of equations are non-linear partial differential equations for unknowns of velocity and pressure. The stress tensor in the last term is represented in terms of the viscosity and strain rate tensor to arrive at the Navier-Stokes equations. The conservation of energy equation can be included as well for problems involving thermal effects. Compressible flow problems would also include density as a variable with a required equation of state. Unfortunately, an analytical solution for all but the most simple flows is, in general, not available. The alternative is an approximate solution using a discrete representation of these differential equations over a grid on points in space and time, the result is an algebraic set of equations that can be solved for the unknown variables.

CFD packages have been developed commercially and have grown to be very powerful, and widely used. Prior to their development extensive experimental efforts were needed, as well as using simplified models for practical solutions. Research continues to advance both CFD, as well as what are known as lower-order models, while trying to minimize the "computational cost".

Since fluid mechanics is ubiquitous in a large number of applications, such as geophysical flows, biological and biomedical flow situations, chemical reactions and combustion situations, etc. CFD has becomes a powerful tool that can be used across many disciplines. Specific application of CFD is extensive, largely due to improved computing power allowing for greater accuracy and shorter times to obtain solutions. CFD is often used to simulate the flow in complex geometries. For instance, it can be used to study the steady and transient effects of moving surfaces (such as propellers, or control flaps on airplanes) as well as fuel and oxidizer inject into combustion chambers. It is also used for weather predictions, pollution analysis, ocean mixing, avalanche prediction, arterial blood flows, and a whole host of other areas.

In the solution to the Navier-Stokes Equations it is possible to identify the velocity field (over space and time) as well as the pressure distribution. These together allow the calculation of forces by integration of the local pressure at an object/fluid interface, as well as calculating the local wall shear stress and then integrating that over the interface as well. With the solution to the energy equation the temperature field and the local distribution of heat flux can be found.

An advantage of CFD when compared with experimental alternatives is the ability to readily evaluate performance without needing a physical model. Parameters can typically be changed more quickly to provide large data bases of information. However, care must be taken to account for the fact that these results are not exact solutions, the sensitivity to the mathematical methods used to discretize the equations to overall accuracy needs to be well understood. Most often experimental verification is an important part of using CFD analysis.

How CFD Works

Since the goal of using CFD is to replace differential equations with algebraic approximations, which can be computationally solved using numerical methods, a grid is formed over the domain of interest to calculate variables of discrete points. Variables are functions of both space and time, with the associated differential terms in the governing equations, consequentially both time and space need to be discretized, and small finite changes over time and space are used to represent derivatives.

The result is a huge number of unknowns which represent the velocity and pressure at every discrete point in the domain that has been set. If a three-dimensional transient problem is being studied, then there most likely needs to be a huge number of unknowns (velocity and pressure over all space for all time of interest). So grid points in space have time dependent variables at each point and the solution has values at each time for each variable at a location. A small grid space of 1000 elements in each of the three coordinates and for 1000 second duration would represent 10^{12} data points for each variable of interest. If information at points other than at the given grid are desired they may be interpolated as necessary, but again this will introduce some additional level of error. So the CFD goal is to solve a very large set of algebraic equations written for each discrete position versus time within the flow. As can be imaged the computational efforts can become enormous. Below is an image of a grid developed to study the flow around an airfoil that is oscillating (heaving and pitching) in order to evaluate the aerodynamic forces on the foil with an application of using this motion in a freestream velocity to extract power from the wind.

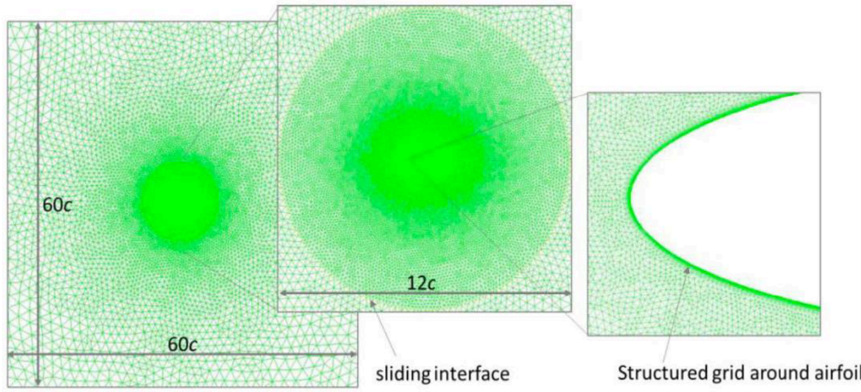

Fig 11.1 Grid used for aerodynamic study of an oscillating airfoil. Shown are three imbedded domains, the first on the left shows the entire flow domain analyzed. The middle image zooms in on the domain around the airfoil (the airfoil is so small it can not be seen here), the grid size is getting progressively smaller and this subregion heaves and rotates within the outer grid. On the right is the region around the tip of the airfoil, even in this region the grid near the airfoil surface is difficult to see. From MS Thesis of Vickie Ngo, School of MIME Oregon State University.

The Finite Difference Method

An example of applying finite differencing to a simple space dependent problem is shown below, taken from notes generated by Bhaskaran and Collins. Start with the differential equation given by:

$$\frac{du}{dx} + u^m = 0; \quad 0 \le x \le 1; \quad u(0) = 1$$

where "m" is a constant parameter and here we set $m = 1$ (resulting in a linear equation). The selected grid is given below where subscripts on x represent different locations in space with four x locations shown along the x coordinate (the distance between points is constant here and given as Δx:

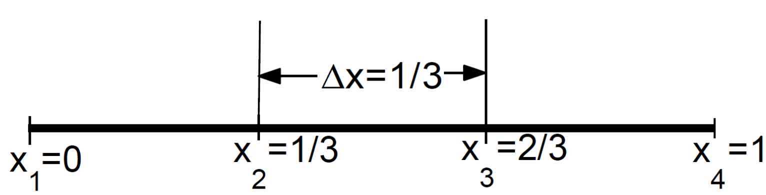

The equation could be evaluated at each location x_i as:

$$\left(\frac{du}{dx}\right)_i + u_i = 0$$

where the subscript i represents the value at grid point $\mathbf{x_i}$. An expression for $(du/dx)_i$ in terms of u at neighboring grid points can be obtained from a Taylor series of $\mathbf{u_{i-1}}$:

$$u_{i-1} = u_i - \Delta x \left(\frac{du}{dx} \right)_i + O\left(\Delta x^2\right)$$

Rearranging gives

$$\left(\frac{du}{dx} \right)_i = \frac{u_i - u_{i-1}}{\Delta x}$$

Since the Taylor series is truncated after the first derivative there is an error introduced on the first derivative that is of order of the square of the size of the grid, $(\Delta \mathbf{x})^2$. This illustrates the importance of the size of the grid. This error is the "truncation error". The governing differential equation can be approximated as:

$$\frac{u_i - u_{i-1}}{\Delta x} + u_i = 0$$

This resulting algebraic equation for u_i simulates the original differential equation but with the truncation error incorporated into it. The error could be reduced by making the grid spacing smaller. Note that an equation of the above form can be written for each grid point in space, resulting in the same number of equations as there are unknown values of the variable, u_i. The system of equations would then be solved for all of the unknowns by applying the necessary boundary conditions.

It should be noted that an alternate approach to discretize the governing equations is the Finite volume method. This method provides discrete variable equations, similar to the finite difference method by forming "cells" or small control volumes as seen in the above figure. The conservation equations are written for each cell assuming single valued variables at the faces of each cell. This is a powerful method that has advantages over the finite difference method. But the net result is still a system of equations for the unknown variables for each cell.

System of Equations

As mentioned above we have a system of equations, one for each grid point. However, some of these grids will be at boundaries, in this example they may be at grid points "1" or "4". Since boundary conditions are needed to be satisfied, they are inserted into the set of equations as known values at these points. Our example is a first order differential equation requiring one boundary condition, which may be at x_1.

Consequently, there are unknowns of grid points 2, 3 and 4, with a known value at 1. The set of equations now becomes just three equations. In matrix form the equation set becomes:

$$\begin{bmatrix} 1 & 0 & 0 & 0 \\ -1 & 1+\Delta x & 0 & 0 \\ 0 & -1 & 1+\Delta x & 0 \\ 0 & 0 & -1 & 1+\Delta x \end{bmatrix} \begin{bmatrix} u_1 \\ u_2 \\ u_3 \\ u_4 \end{bmatrix} = \begin{bmatrix} 1 \\ 0 \\ 0 \\ 0 \end{bmatrix}$$

Note that here the boundary condition equation is included in the matrix. This need not be required by simplifying this to three equations with the boundary condition included in the equation for $\mathrm{u_2}$. That is to say the first row and first column in the matrix would be excluded from the matrix above with the value of $\mathrm{u_1}$ input into the first row of the vector on the right hand side as a known value of "1".

In this simple example it is easy to invert the matrix and calculate the values of $\mathrm{u_i}$ for a given value of $\Delta\mathrm{x}$. It is also possible to see that there is an exact solution to this problem, $\mathrm{u} = \exp(\text{-x})$. It is left to the reader to compare results at the discrete points and to show that the difference between exact and approximated values decrease with decreasing values of $\Delta\mathrm{x}$. It is also seen that as $\Delta\mathrm{x}$ is decreased the number of discrete points increases and the calculation become more complex and time consuming.

This leads to the issue of "grid convergence" – as the grid size is reduced one may expect that the solution would converge to the exact solution. This is illustrated in the figure below, from the notes of Bhaskaren and Collins based on the example above.

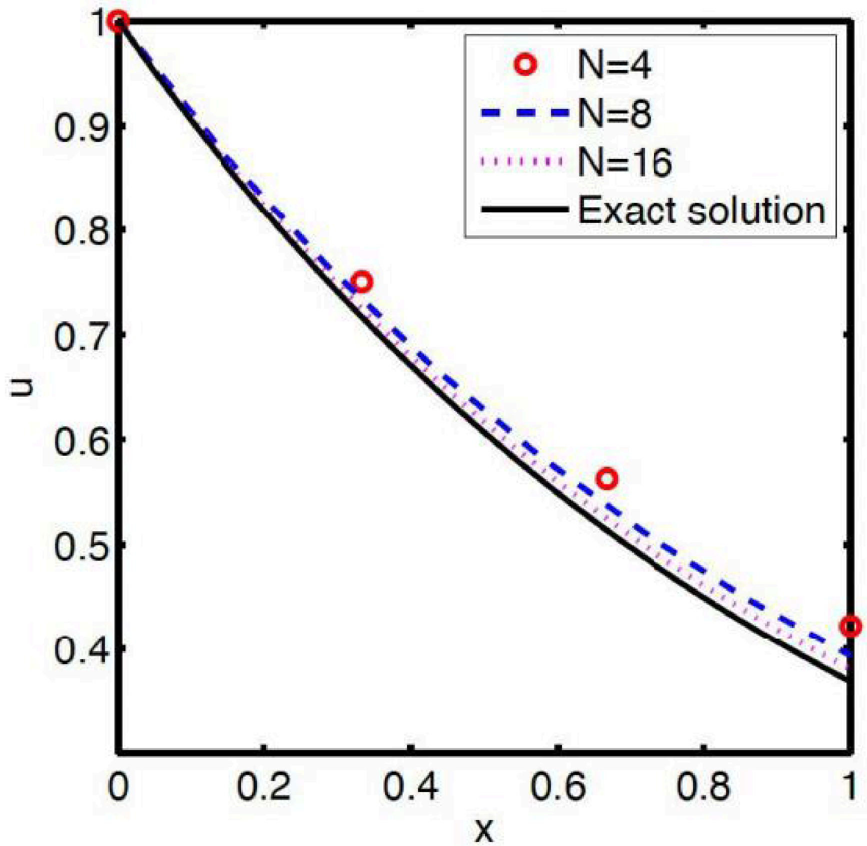

Fig 11.2 This figure shows how the predictions using the finite difference approximations become closer to the exact analytical solution as the grid size decreases (or number of discrete points, N, within the domain increases). Note also that the error varies with the specific x location. As the error decreases with the decreased grid size a "grid convergence" is observed ultimately becoming so small it is not of direct interest to the solution – a "grid independent solution".

Nonlinear Effects

The above example can be expanded in scope by changing the value of the exponent "m" from the value of one. If $\mathrm{m} = 2$ then the second term is nonlinear, u^2. This type of governing equation, with linear and nonlinear terms, is in fact similar to the Navier-Stokes equations where the $(\vec{V} \cdot \nabla)\vec{V}$ term is nonlinear.

Going through the same exercise of discretizing the differential term of our example it is shown that the only change to the finite difference algebraic equation is u^2. This could lead to multiple possible solutions. One way to solve this type of system of equations is to "linearize" the equations. This is done by iteration around a guessed value of the variable. That is we assume u_i^2 is $(u_{gi})\,(u_i)$ which is then the product of two different variables, the guessed value u_{gi} and u_i. The guessed value is iterated upon until convergence is reached. To do this the difference between the actual and guessed value of u_i is denoted as $\Delta u_i = (u_i - u_{gi})$, squaring both sides and solving for u_i^2 results in:

$$u_i^2 = u_{g_i}^2 + 2u_{g_i}\Delta u_i + (\Delta u_i)^2$$

Noting that on the right the second term is much larger than the third, since it is expected that $u_{gi} > \Delta u_i$, the last term is then neglected. The final expression for u_i^2 is:

$$u_i^2 \simeq 2u_{g_i}u_i - u_{g_i}^2$$

where this expression has the inherent error of $O\left(\Delta u_i^2\right)$. The right hand side is inserted into the governing equations and the iteration is then applied to the guess values of u_{gi}. An initial guess for u_{gi} is made and solutions are obtained for u_i, for the now linearized problem. The solution is compared with the guessed values u_{gi}, and if different the updated u_i is used as the new u_{gi}. This is repeated until the difference between u_i and u_{gi} becomes acceptably small. So the solution method is one of solving a linear equation based on an iteration of the linearized term expression.

The "residual" can be defined as the difference between the solution and the guess used at an iteration. An overall residual for the domain can be compiled from residuals at each point as:

$$R \equiv \sqrt{\frac{\sum_{i=1}^{N}\left(u_i - u_{g_i}\right)^2}{N}}$$

This provides a measure, on average, of how well all of the grid points are converging. This residual can be scaled with some measure of the value of u throughout the domain, such as the mean value, to provide a measure of residual as a fraction of the mean. Other scaling options are also possible. The "convergence criteria" is measured by the scale residual. In other words a convergence criteria can be set to some small number and the problem is run until that criteria is met. Students can test convergence for this problem, as well as with the exact solution for $m = 2$ of $u = 1/(1+x)$.

Numerical Stability

The convergence towards a solution is highly dependent on the form of the governing equation and boundary conditions. Convergence may be very fast or slow or never and depends on the numerical solution scheme being used. A "stability analysis" can inform the user what to expect. When a solution does not converge (diverges) the method is "unstable". A stable method is not necessarily going to results in an accurate solution.

A steady state problem can be solved in different ways. An iterative solution could be used by guessing initial values and trying to converge towards a stable solution. Alternatively, the problem could be solved as a transient problem and started from some initial condition and the transient equations solved over discrete time steps until a steady (non-changing) value is reached. For transient solutions the time step is critical in determining stability. A time step that is too large (which is numerical scheme dependent) can cause the solution to diverge.

Explicit and Implicit Schemes

Whether a method is explicit or implicit is a distinction based on how variables in the equation are solve. Obviously, for a transient problem there is a time dependent term, such as a time derivative. Discretizing this term results in the ratio of the change of variable to the time step interval selected: $\left(u_1^{n+1} - u_1^n\right)/\Delta t$, where the superscript on the variable u represents values at time steps n+1 and n, and Δt is the time interval between time steps. If all other terms in the equation express the variables at time step "n" the only unknown is the variable at the new time step, n+1, since presumably the solution has been found at time step n (or is the initial condition). This is an explicit solution for the variable at time step n+1. These types of equations are stable under a certain constraint on time step and spatial step size conditions. The Courant number is a parameter used to indicate stability and is defined as $C = K\Delta t/\Delta x$ where the proportionality constant, K, is related to parameters in the problem and has units of distance per time. The value of C is nondimensional and is typically limited to numbers less than one for stability and implies that as the grid size is made larger the allowable time step size can also increase to remain stable. Although large time steps allow for less computational effort, the problem is that as the time step and grid size get large the error also grows.

As an alternative method, the time derivative could be written as a time derivative between time steps n and n-1 (backwards differencing) where the solution is known at n-1 and solved at time step n. Here all other terms in the equation have their variables identified at time step n. In this form the n-1 variables are known and the n variables unknown, and there are multiple unknowns per equation. Each equation can not be solved explicitly but rather a system of equations exist that must be solved implicitly through the entire system of equations for all of the grid points.

In contrast to the above constraint on the time step for explicit solutions through the Courant number, implicit solution schemes tends to be stable for much larger time steps. Note that this does not imply that it is accurate, however, and care must be taken in reaching acceptable levels of numerical errors.

Turbulence Modeling

Fluid flows are often classified as either laminar or turbulent, as discussed in the previous chapters, with a critical Reynolds number often defining where a transition tends to occur. The impact of flows being laminar or turbulent can be enormous. In particular there are consequences relative to wall friction, drag and lift forces, mixing within a fluid, dispersion of species within the flow and heat transfer rates that occur within the fluid and many others. Turbulence is characterized by fluctuations in time and space. The added complexity of turbulent fluid motion occurs over a very wide range of fluctuating time and length scales makes the flow extremely complicated (and interesting!).

The fluctuating variables over time and space give rise to added complexities associated with attempts to solve the Navier-Stokes equations. Using very small time difference, and very small spatial difference to resolve the time and space derivatives allows one to solve the governing equations and basically unravel the turbulent motion. The problem is that these scales become extremely small, particularly for flows with large values of Reynold number. Solutions that use sufficiently small time steps and spatial resolution are called "direct numerical simulations" or *DNS* and are very computationally expensive. Computing power is no where near sufficient to apply these solutions to reasonably large flows in an economic manner.

An alternative to DNS is to evaluate the time averaged mean quantities only. The need to analyze time averaged turbulent flows has driven the development of highly sophisticated turbulence models so that the need to resolve the very small fluctuations of motion over time and space are not as important. These models must determine the effects of the fluctuating turbulence on the mean flow and incorporate these into the solution for the mean flow variables of velocity and pressure.

The approach to turbulence modeling has evolved over the years as time average representation of the Navier-Stokes equations. As discussed previously, the Reynolds stress, which contains information on the fluctuating velocity, is a consequence of time averaging the nonlinear Navier-Stokes equation, specifically the advection term. This term appears as the time averaged product of fluctuating velocity components (since it is nonlinear). This time average process is called Reynolds averaging where each variable is taken to be the sum of its time averaged mean value and a fluctuating value that varies with time (or $u\left(t\right)=U+u'\left(t\right)$ with U being the time averaged value of the velocity and u' the fluctuating value about the time averaged value). The mean value is time independent and the fluctuating value varies with time, but has a time average of zero. When each term in the Navier-Stokes equation is time averaged, all fluctuating terms become zero except the nonlinear advection term. Without derivation here we show that the resultant advection term contains the following (where the overbar is the time average):

$$\frac{\partial\left(\rho\overline{u_i'u_j'}\right)}{\partial x_j}$$

The following model is used:

$$\rho\overline{u_i'u_j'} = 2\mu_t S_{ij} - \frac{2}{3}\rho k\delta_{ij}$$

$$S_{ij} = \frac{1}{2}\left(\frac{\partial U_i}{\partial x_j} + \frac{\partial U_j}{\partial x_i}\right); \quad k = \frac{1}{2}\overline{u_i'u_i'}$$

The terms in this model are explained as follows. The advection term is the spatial derivative of $\left(\rho\overline{u_i'u_j'}\right)$, which has units of N/m^2 per volume of fluid in SI units, equivalent to a stress per volume, the so called Reynolds stress or turbulent stress. Since this term appears as a spatial derivative of a stress, a possible model would be to mimic the laminar stress model and express the "turbulent stress" as the product of a "turbulent viscosity", μ_t, times the strain rate tensor, S_{ij}, shown above. The model also includes the parameter k, known as the turbulent kinetic energy. In using this model the turbulent stress is replaced by an unknown turbulent viscosity μ_t and k. The turbulent viscosity is dependent on the turbulence in the flow, rather than just the fluid as in the laminar case. A model needs to be developed to determine both the turbulent viscosity and turbulent kinetic energy. A model for these turbulent parameters is not easy and there are several that have been proposed.

If the turbulent viscosity is to model the added mixing of momentum caused by the turbulent flow, then one approach is to relate this to the turbulent energy of the turbulence, k. This energy, which is the energy per mass of fluid, is defined as one half of the time average of the square of the fluctuating velocity. The greater the amplitude of the fluctuating velocity the greater the turbulent kinetic energy.

Also, the turbulent viscosity is assumed to be dependent on how much the turbulent kinetic energy is dissipated by the friction occurring with the surrounding fluid. The "turbulent dissipation", ε, is defined as the rate of loss of tke and has units of energy per time per mass of fluid, or m^2/s^3.

If the assumption is made that $\mu_t = \rho\nu_t$ (where ν_t is the turbulent kinematic viscosity) and that $\nu_t = f(k, \varepsilon)$ then by dimensional analysis (where the units of the turbulent kinematic viscosity, ν_t are m^2/s) a form of this function could be: $\nu_t = C_\mu\left(k^2/\varepsilon\right)$, where C_μ is an empirical nondimensional constant of 0.09. Taking this approach the problem as reverted to knowing the local distribution of k and ε and from this being able to calculate ν_t at each point in the flow and then use this to calculate the Reynolds stress from the above model. This stress can be inserted into the Navier-Stokes equations and solved for the time averaged mean velocity and pressure.

To complete the model two additional transport equations, one each for k and ε, are derived from the time varying Navier-Stokes equations. The result is two differential equations that need to be solved at each grid location (or cell if using a finite volume method). This is known as the two equation turbulence model. This results in significant computation effort added to the solution of the mean Navier-Stokes equations (one for each coordinate direction).

There are a number of similar turbulence models that are available in most commercial software packages. The “best” one to use depends on the flow conditions and the accuracy is typically dependent on the computational expense. It is very important to be aware of limitations of the various models which is usually described for the software user in these commercial software packages. The result is a solution for the mean, time averaged, variables.

CREATIVE COMMONS LICENSE

RECOMMENDED CITATIONS

APA outline:

Source from website:

- (Full last name, first initial of first name). (Date of publication). Title of source. Retrieved from https://www.someaddress.com/full/url/

Source from print:

- (Full last name, first initial of first name). (Date of publication). Title of source. Title of container (larger whole that the source is in, i.e. a chapter in a book), volume number, page numbers.

Examples

If retrieving from a webpage:

- *Berndt, T. J. (2002). Friendship quality and social development.* Retrieved from insert link.

If retrieving from a book:

- Berndt, T. J. (2002). Friendship quality and social development. *Current Directions in Psychological Science, 11*, 7-10.

MLA outline:

Author (last, first name). Title of source. *T*itle of container (larger whole that the source is in, i.e. a chapter in a book), Other contributors, Version, Number, Publisher, Publication Date, Location (page numbers).

Examples

- Bagchi, Alaknanda. "Conflicting Nationalisms: The Voice of the Subaltern in Mahasweta Devi's Bashai Tudu." *Tulsa Studies in Women's Literature*, vol. 15, no. 1, 1996, pp. 41-50.
- Said, Edward W. *Culture and Imperialism.* Knopf, 1994.

Chicago outline:
Source from website:

- Lastname, Firstname. "Title of Web Page." Name of Website. Publishing organization, publication or revision date if available. Access date if no other date is available. URL .

Source from print:

- Last name, First name. *Title of Book*. Place of publication: Publisher, Year of publication.

Examples

- Davidson, Donald, *Essays on Actions and Events.* Oxford: Clarendon, 2001. https://bibliotecamathom.files.wordpress.com/2012/10/essays-on-actions-and-events.pdf.
- Kerouac, Jack. *The Dharma Bums.* New York: Viking Press, 1958.

VERSIONING

This page provides a record of changes made to this publication. Each set of edits is acknowledged with a 0.01 increase in the version number. The exported files, available on the homepage, reflect the most recent version.

If you find an error in this text, please fill out the form at bit.ly/33cz3Q1

Version	Date	Change Made	Location in text
1.0	**9/16/2021**	**Publication**	
1.01	12/09/2021	Equation updates	Introduction to turbulence effects
1.02	6/28/2022	Equation updates	Potential Flow Basics
1.03	7/15/2022	Equation updates, copy updates	Bernoulli Equation, Potential Flow Basics, Introduction to Viscous Flows
1.03	7/15/2022	Equation updates	Potential Flow Basics
1.03	7/15/2022	New publication, copy updates	Introduction to Turbulence Effects, Brief Introduction to CFD Basics
1.03	7/15/2022	Format updates	All
2.0	9/19/2022	Equation updates, Format updates	All
2.01	11/7/2022	Equation updates	Bernoulli Equation
2.02	11/29/2022	Equation updates	Boundary Layer Flows, Integral Boundary Layer Relationships